

1-1-1994

## Theoretical and experimental analysis of the thermoacoustic refrigeration

Amritraj B Singh

*University of Nevada, Las Vegas*

Follow this and additional works at: <https://digitalscholarship.unlv.edu/rtds>

---

### Repository Citation

Singh, Amritraj B, "Theoretical and experimental analysis of the thermoacoustic refrigeration" (1994). *UNLV Retrospective Theses & Dissertations*. 425.

<http://dx.doi.org/10.25669/f9lb-obt3>

This Thesis is protected by copyright and/or related rights. It has been brought to you by Digital Scholarship@UNLV with permission from the rights-holder(s). You are free to use this Thesis in any way that is permitted by the copyright and related rights legislation that applies to your use. For other uses you need to obtain permission from the rights-holder(s) directly, unless additional rights are indicated by a Creative Commons license in the record and/or on the work itself.

This Thesis has been accepted for inclusion in UNLV Retrospective Theses & Dissertations by an authorized administrator of Digital Scholarship@UNLV. For more information, please contact [digitalscholarship@unlv.edu](mailto:digitalscholarship@unlv.edu).

## **INFORMATION TO USERS**

**This manuscript has been reproduced from the microfilm master. UMI films the text directly from the original or copy submitted. Thus, some thesis and dissertation copies are in typewriter face, while others may be from any type of computer printer.**

**The quality of this reproduction is dependent upon the quality of the copy submitted. Broken or indistinct print, colored or poor quality illustrations and photographs, print bleedthrough, substandard margins, and improper alignment can adversely affect reproduction.**

**In the unlikely event that the author did not send UMI a complete manuscript and there are missing pages, these will be noted. Also, if unauthorized copyright material had to be removed, a note will indicate the deletion.**

**Oversize materials (e.g., maps, drawings, charts) are reproduced by sectioning the original, beginning at the upper left-hand corner and continuing from left to right in equal sections with small overlaps. Each original is also photographed in one exposure and is included in reduced form at the back of the book.**

**Photographs included in the original manuscript have been reproduced xerographically in this copy. Higher quality 6" x 9" black and white photographic prints are available for any photographs or illustrations appearing in this copy for an additional charge. Contact UMI directly to order.**

# **UMI**

A Bell & Howell Information Company  
300 North Zeeb Road, Ann Arbor, MI 48106-1346 USA  
313/761-4700 800/521-0600



# **THEORETICAL AND EXPERIMENTAL ANALYSIS OF THERMOACOUSTIC REFRIGERATION**

**by**

**Amritraj B. Singh**

**A thesis submitted in partial fulfillment  
of the requirements for the degree of**

**Master of Science**

**in**

**Mechanical Engineering**

**Department of Mechanical Engineering  
University of Nevada, Las Vegas  
August 1994**

**UMI Number: 1361101**

---

**UMI Microform Edition 1361101**  
**Copyright 1995, by UMI Company. All rights reserved.**

**This microform edition is protected against unauthorized  
copying under Title 17, United States Code.**

---

**UMI**

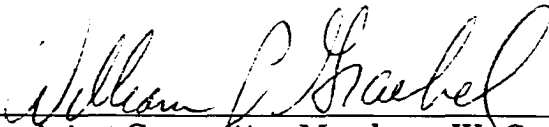
**300 North Zeeb Road  
Ann Arbor, MI 48103**

The thesis of Mr. Amritraj B. Singh for the degree of Master of Science in Engineering (Mechanical Engineering) is approved.



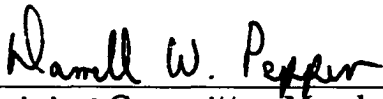
---

Chairperson, R. F. Boehm, Ph.D.



---

Examining Committee Member, W. Graebel, Ph.D.



---

Examining Committee Member, D. Pepper, Ph.D.



---

Graduate Faculty Representative, M. Karakoujian, Ph.D.



---

Dean of Graduate College, Ronald W. Smith, Ph.D.

University of Nevada, Las Vegas  
August 1994

## **ABSTRACT**

The thermoacoustic theory is studied in detail and its application to refrigeration is analyzed. This new refrigerator which uses resonant high amplitude sound in inert gases to pump heat will be described. It will be seen that without any moving parts, except the driver (speaker diaphragm), this refrigerator is as efficient as other refrigeration systems. An experiment is designed with all the major parts manufactured and fabricated in the lab. The results of the experiments are seriously effected due to the leakage of helium. Detailed recommendations are made which will help prevent similar design problems. In addition, numerical simulation was performed using a FORTRAN program to examine the variation of various parameters with frequency and acoustic pressure.

## CONTENTS

ABSTRACT.....	iii
LIST OF FIGURES.....	vi
ACKNOWLEDGEMENTS.....	viii
CHAPTER 1 INTRODUCTION.....	1
Introduction.....	1
History.....	2
CHAPTER 2 LITERATURE REVIEW.....	6
Introduction.....	6
Thermoacoustics.....	6
Heat Transfer in Oscillating Fluids.....	17
CHAPTER 3 ANALYSIS.....	26
Introduction.....	26
Theory.....	26
Analysis.....	29
Physical Description.....	50
CHAPTER 4 EXPERIMENTAL APPARATUS AND DESIGN.....	54
Introduction.....	54
Primary Components.....	57
Secondary Components.....	68
Instrumentation.....	75
CHAPTER 5 EXPERIMENT AND RECOMMENDATIONS.....	78
Introduction.....	78
Assembly.....	78
Test Run.....	79
Recommendations.....	80
Conclusion.....	85
NOMENCLATURE.....	88
BIBLIOGRAPHY.....	90
APPENDIX A FORTRAN PROGRAM.....	93
APPENDIX B.....	98

APPENDIX C HELIUM.....	100
APPENDIX D THEORY OF ACOUSTICS.....	102

## LIST OF FIGURES

Fig. 1. A profile of the thermoacoustic system used by Wheatley.....	10
Fig 2. Schematic of a three plate thermoacoustic couple with support structure and with one thermoelectric couple mounted with junctions at C and H to sense the temperature difference across the couple. (Wheatley et al., 1983).....	12
Fig. 3. Schematic diagram of a one quarter wavelength, thermoacoustic refrigerator used by Garrett (1991). The dotted line denotes the pressure profile inside the tube.....	15
Fig. 4. An expanded view of co-ordinate system used for the analysis with plate and spacing thicknesses.....	29
Fig. 5. This plot shows the variation of energy flux, $H$ (Watt) and wavelength, $\lambda$ (m) with frequency, $f$ (Hz) at mean temperature.....	41
Fig. 6. This plot shows the variation of acoustic power, $W$ (Watt) with frequency, $f$ (Hz) at the parameters given in fig. 5.....	42
Fig. 7. This plot shows the variation of COP with frequency, $f$ (Hz) at the parameters given in fig. 5.....	43
Fig. 8. This plot shows the variation of energy flux, $H$ (Watt) with pressure amplitude, $P_1$ (Pascal) at the parameters given in fig. 5.....	44
Fig. 9. This plot shows the variation of acoustic power, $W$ (Watt) with pressure amplitude, $P_1$ (Pascal) at the parameters given in fig. 5.....	45
Fig. 10. This plot shows the variation of COP with pressure amplitude, $P_1$ (Pascal) at the parameters given in fig.5.....	46
Fig. 11. This plot shows the variation of velocity, $u_1$ with pressure $P_1$ (Pascal) at the parameters given in fig. 5.....	47
Fig. 12. This plot shows the variation of energy flux, $H$ (watt) with the tube radius, $R$ (m) At the parameters given in fig.5.....	48
Fig. 13. This plot shows the variation of acoustic work, $W$ (Watt) with tube radius, $R$ (m) at the parameters given in fig. 5.....	49

Fig. 14. Thermodynamic cycles with state points and process lines. (A) shows the cycle with entropy and temperature and (B) shows the Pressure and volume changes.....	51
Fig. 15. Developed model of the refrigerator. (A) is the tube of $1/4$ length with stack and the cold (C) and hot (H) sides. (B) is the tube with $1/2$ length. a. shows the velocity profile and b. shows the pressure profile.....	53
Fig. 16. An overview of the thermoacoustic system used for the experiment with all the major parts numbered.....	55
Fig. 17. The main resonator section with dimensions.....	59
Fig. 18. Heat exchanger sections with all details and dimensions in two different views.....	61
Fig. 19. Heat exchanger with dimensions in two different views.....	62
Fig. 20. The construction of the stack roll. (A) Porous aluminium jig plate with tooth like projections, (B) spacer strings (monofilament fish line) applied to the surface of the film on the alignment jig. The strings are cut along the length at point.....	66
Fig. 21. Acrylic flanges in two different views.....	69
Fig. 22. End cap with thread connection for the vacuum pump and helium.....	71
Fig. 23. Speaker casing shown in two different views with the threads drilled at positions shown by 'a'.....	72
Fig. 24. Speaker cover in two different views with connection shown for pressure equalizer.....	74
Fig. 25. Block diagram showing various components in the experimental thermoacoustic system.....	76

## ACKNOWLEDGEMENTS

I would like to acknowledge and express my gratitude to my advisor Dr. R. F. Boehm, Chairman of Mechanical Engineering Department, University of Nevada, Las Vegas, for his motivation, guidance and concern throughout my research work and education.

I would also like to thank Dr. William Graebel for his substantial help in the design of the experimental setup. I am also indebted for the aid provided to me by the Department of Mechanical Engineering.

I am grateful to all my professors and friends for their encouragement.

I would also like to acknowledge my parents and family members for their moral support.

## **CHAPTER 1**

# **INTRODUCTION**

## **INTRODUCTION**

The credit for the insight into the topic of thermoacoustics goes to Kirchhoff, whose work has been considered by Rott as mentioned by Hofler (1986). Kirchhoff dealt with the thermal diffusion in sound waves in a tube. This topic has been discussed in many basic acoustic textbooks. Merkli and Thomann (1975) had successfully understood and described the thermoacoustic process. When there is an acoustic standing wave in a duct with walls at a uniform temperature, there occurs a net heat transport along the duct walls. Heat is actually transported from a region near the velocity antinode of the standing wave to the region near the adjacent pressure antinode. This phenomenon was called 'thermoacoustic streaming' by Rott.

There are two classes of heat engines: prime movers and heat pumps. In a prime mover, heat flows through the engine from high to low temperature. In heat pumps, the reverse of the above occurs, i.e., work is absorbed by the engine, resulting in the pumping of heat

from low temperature to high temperature. Since the Carnot's efficiency is the highest efficiency that a prime mover or heat pump can achieve, it is the desire to achieve this efficiency that a heat engine is designed. But a practical heat engine is designed against needs of low cost, high reliability, safety, compactness, easily mass producible.

In the light of above mentioned criteria, the thermoacoustic heat engine has been of moderate priority. Since the principle qualities of a thermoacoustic heat engine, which is the subject of this thesis (thermoacoustic refrigerator/heat pump), are reasonable efficiency and extreme simplicity, it is possible that the thermoacoustic would be put to practical use shortly.

The thermoacoustic engines achieve their simplicity by using no moving parts (except for the driver), no exotic materials, and no close tolerances. In the demonstration experiment conducted by Swift (1987), he generated loud sound using the heat from a propane flame. The construction and working of this interesting prime mover will be covered later in the chapter.

## **HISTORY**

Shortly after their introduction, chlorofluorocarbons (CFCs) used as working fluids in a vapor compression (Rankine) refrigeration cycle became dominant in almost all small and medium scale food refrigerators and building air conditioning applications. CFCs were recently discovered to be destroying the Earth's stratospheric protective ozone layer and their production will be halted by the year

2000. Though this seems to be a difficult proposition, one possible alternative to the CFCs is called "Thermoacoustic Refrigeration". Substitute compounds HCFCs and HFCs have problems associated with their pollution potential, their toxicity, and their incompatibility with lubricants.

In 1777 Byron Higgins conducted experiments in which acoustic oscillations in a large pipe were excited by suitable placement of a hydrogen flame inside (Swift, 1987). His research evolved into pulse combustion, which was applied in German V-1 rockets used in World War II and the residential pulse combustion furnace introduced by Lennox, Inc. in 1982.

About a century ago glassblowers noticed that when a hot glass bulb was attached to a cool glass tubular stem, the stem tip emitted sound, which was quantitatively investigated by Sondhauss (Wheatley, *et al.*, 1986). An investigation was conducted as to the relation of the pitch of the sound to the dimension of the apparatus.

Taconis oscillation is another variant of the thermoacoustic prime mover (Swift, 1987). These oscillations, often of high amplitude, can occur when a gas filled tube reaches cryogenic temperatures from room temperature. According to Swift (1987), Gifford and Longworth produced refrigeration using a pulse tube refrigerator by applying very low frequency, high amplitude pressure oscillations to a gas-filled tube. Later Merkli and Thomann observed slight cooling around the velocity antinode of the gas resonating in a simple cylindrical resonator, and presented an accurate theory of the effect.

The working of the Rijke tube has been known and the interaction between acoustics and thermodynamics was recognized long ago. Also the fact that speed of sound was determined either by adiabatic or isothermal compressibility of air was the point of discussion between Newton and Laplace. But it has been understood that the thermal gradients can lead to the production of sound. The reverse process of thermoacoustic heat pumping has been the focal point only in the last decade. The new approach to thermoacoustic refrigeration, discovered in the early 1980s, uses high intensity sound waves to pump heat in an inert gas medium.

Practically all the known heat and mass transfer processes develop more rapidly in an acoustic field than when traditional technology is employed (*e.g.*, combustion in the car engine). This means that the acoustic waves can highly exaggerate heat transfer phenomena, *e.g.*, vibratory combustion appliances are characterized by greater combustion intensity in the combustion chamber, improved heat transfer to the chamber walls, and hence greater overall efficiency and power. This can be seen in the rocket engine in which the high frequency self oscillations can lead to the destruction of the engine itself.

The known fundamental heat engine cycles, such as the Carnot cycle, assumes that the steps in the cycle are reversible. Such analysis using the first and second laws of thermodynamics, lead to the limiting (highest practical values) of the efficiencies of prime movers and the COP of refrigerators. But these limiting values and the reversibilities are never achieved in the real systems due to the irreversibilities, thermal diffusion and viscous dissipation, which

always reduce the performance. These also require the mechanical devices to execute the proper phasing of various cycles. In thermoacoustic engines, the irreversibility due to the imperfect (diffusive) thermal contact between the acoustically oscillating working fluid and a stationary second thermodynamic medium provides the required phasing. This natural phasing has produced heat engine which requires no moving parts other than the self maintained oscillations of the working fluid.

## **CHAPTER 2**

# **LITERATURE REVIEW**

## **INTRODUCTION**

The broad category of studies in thermoacoustics can be divided into two major sections, thermoacoustics and heat transfer effects. Therefore the literature review here is dealt-with separately in two sections.

## **THERMOACOUSTICS**

The detailed thermoacoustic study can be credited to Rott (1969) whose theory seems to be the basis for most investigations in this area of physics and engineering. Much of his work was in the physics of the thermoacoustic heating. His pioneering work was the basis of the investigation done by Hofler.

Rott (1969) investigated Kirchoff's theory. This theory states that a tube closed at one end and open at the other, filled with helium, can oscillate spontaneously when the open end is at the cold temperature (liquid helium temperature, 4 K) and hot at the closed

end (room temperature). In the same paper Rott made some interesting assumptions,

- a) The radial gradient of the acoustic pressure is neglected throughout the tube.
- b) The radial variations of the average temperature and of the viscosity are neglected.
- c) Axial heat conduction in the acoustic wave and friction due to axial gradients are ignored.

A consideration of the stability theory was used to define optimum effectiveness of the driving mechanism (Rott, 1973).

An attempt to calculate the effects of thermoacoustic streaming led to a situation where no closed form solution existed (Rott, 1975).

Calculations made on the effect of an oscillating gas column on the closed end of an isothermal tube showed that the closed end is always heated, i.e., heat flows from the gas to the wall (Rott, 1984). The axial heat flux per unit tube length is proportional to the product of the acoustic pressure and velocity (Rott, 1975). If no heat is removed from the end of the tube, the temperature of the gas and the wall will increase to yield a zero gradient condition (adiabatic). Then the attendant heat flux into the gas is proportional to the temperature gradient in the gas and to the square of the acoustic velocity (Rott, 1975). Though the acoustic velocity and total heat flux vanish at the closed end, the second kind of heat flux vanishes only with the square of the velocity. Thus the heat flux of the second kind cannot compensate for the heat flux of the first kind in the vicinity of the closed end unless the temperature gradient becomes very large. According to Rott the ultimate steady state singularity is obtained by

setting the total resultant heat flux equal to zero. From the above conditions and theory, Rott carried over the calculations with different procedure to determine singularity, based on a heuristic argument set forth by Gifford and Longworth (1984) in connection with the explanation of their pulse tube.

Merkli and Thomann (1975) conducted experiments with the gas filled resonance tube to prove that not only heating, but also cooling of the tube, is possible and these phenomena are not restricted to oscillation amplitudes that generate shocks. These results show cooling in the section of the tube with maximum velocity amplitudes and marked heating in the region of the velocity nodes. A strong dependence on the Prandtl number is also noted. The experimental setup is essentially a tube of constant diameter and length. At one end of the tube, the oscillations are driven by a piston, which performs a simple harmonic motion. The other end of the tube is closed by a shiftable end piece so that different lengths may be set. This end piece contains a pressure transducer which gives a reference signal, which allows an exact determination of the oscillation frequency. The frequency of the piston was adjusted to work between 0-130 Hz and the amplitude 2.85-13.8 mm.

The experiments were conducted with different amplitudes and different frequencies and their thermal effects noted. The results showed that cooling occurs in the region of the velocity antinode if no shocks or, at the shock region boundary, only weak shocks appear. Towards the shock region slight departures of the measurements from the theory appear. According to the author this is not only due to the nonlinearities but also to the appearance of turbulent bursts.

Also the thermal effects are strongest in the shock region. When shocks are absent, the new theory allows an accurate calculation of these effects. Discrepancies arise near resonance owing to nonlinearities and for strong oscillations also owing to turbulence. The occurrence of the turbulence is treated in a separate paper by Merkli and Thomann (1975b). In this paper the heat flux penetrating the tube wall is calculated. The paper clearly indicates that resonance tube can be used as a heat pump.

Wheatley *et al.* (1983) have studied, experimentally and by calculation, some thermoacoustic effects in structures (a stack of thin plates placed inside the cylinder which is closed on one side and open at the other) placed in an acoustically resonant tube containing helium gas (see fig. 1). When the acoustic power is turned on, the part of the stack at the open end is cooled and the closed end is heated with the intermediate positions showing small heating. After some time the temperature difference between the open end and the closed end exceeds 100 °C, with one end below ambient and the other end above ambient. These experiments and their analysis show that the cooling and heating occur because application of acoustic power by the driver causes an average flow of entropy out of the end of the stack closer to the closed end of the tube. The heating effects were studied using an "adiabatic calorimeter" method, in which a stack of three plates is placed with one end very near to closed end of a tube. The plates were made of fibre glass and the tube was made of thick Inconel. Thermocouples were soldered on to the plates to record the temperature. A thermocouple was also fastened to the outside wall of confining tube. The tube was filled with helium gas to

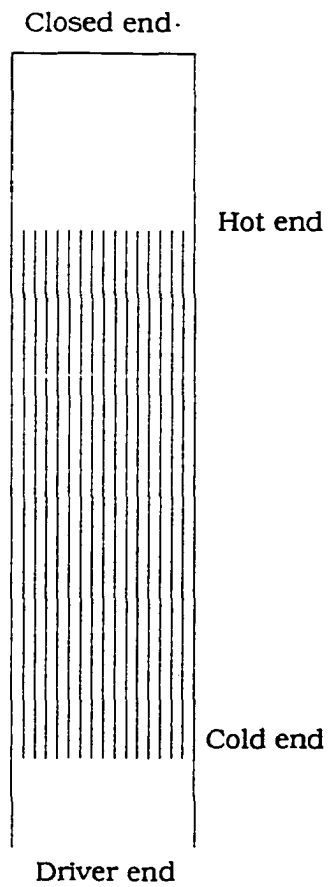


**Fig. 1. A profile of the thermoacoustic system used by Wheatley *et al.***

desired pressure. The material of the plates was changed to copper and stainless steel for comparison. The effect of the plate separation was as critical a parameter as was the positioning of the stack in the tube. The heating rate is sensitive to flow configuration and qualitative changes from simple boundary layer theory begin to show up for plate separation  $d < \delta_v$ , where  $\delta_v = (2\nu/\omega)^{1/2}$  is the viscous penetration depth.

All the variables were broken down into first order and second order (the detailed discussion of the order of the variables is given in the analysis chapter). The first order quantities are solved by taking the fundamental equations and linearising them and substituting the expanded physical variables. The second order solutions (subscript 2) are obtained using the exact fundamental equations, substituting the expanded variables and eliminating all terms with indices that sum to three or more.

The second order acoustic heating rate of the plates per unit area at any point is calculated using a boundary layer approximation and is found to be

$$Q_2 = \frac{1}{4} \omega p_o^2 \frac{\delta_k}{p_m} \{ (\sqrt{\text{Pr}} + \gamma - 1) \left( \frac{1}{2\gamma} \right) \frac{(\gamma(1+\text{Pr}) + (1-\text{Pr})(1+\sqrt{\text{Pr}}))}{(\gamma(1+\text{Pr}) - (1-\text{Pr})(1-\sqrt{\text{Pr}}))} \} \cos \frac{2x}{\lambda} \quad (1)$$

where  $\omega$  is angular frequency,  $\gamma$  is the ratio of specific heats,  $\text{Pr}$  is the Prandtl number -  $\nu/\kappa$ . Here  $\nu$  is the kinematic viscosity and  $\kappa$  is the thermal diffusivity, equal to the ratio of thermal conductivity ( $k$ ) to specific heat per unit volume  $\rho c_p$ ,  $\delta_k = (2\kappa/\omega)^{1/2}$  is the thermal penetration depth,  $P_m$  is the mean pressure,  $P_o$  is the amplitude of

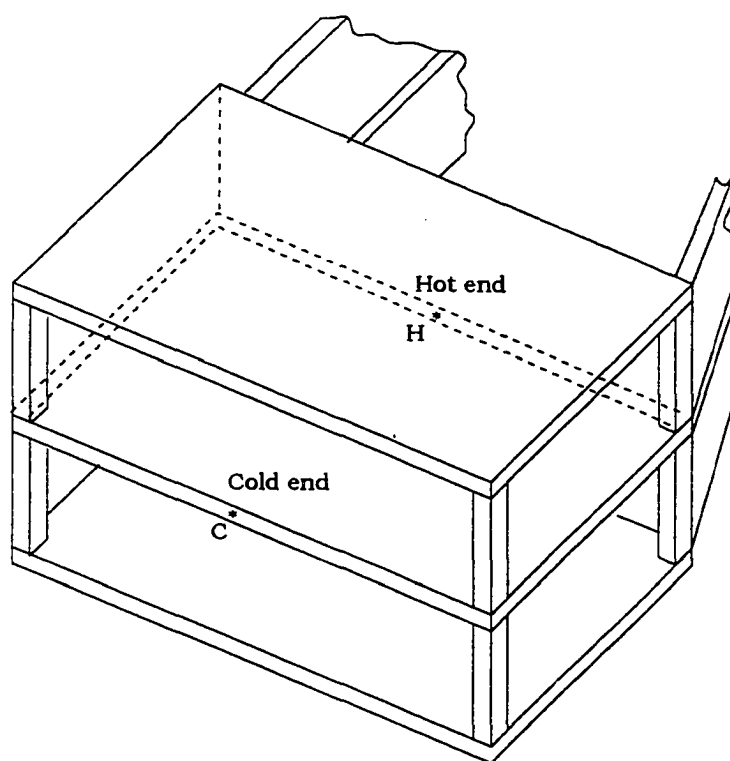


**Fig 2. Schematic of a three plate thermoacoustic couple with support structure and with one thermoelectric couple mounted with junctions at C and H to sense the temperature difference across the couple. (Wheatley *et al.*, 1983).**

the dynamic pressure at the closed end,  $x$  is the longitudinal distance measured from zero at 'H' (see fig. 2), the end closest to the closed end of the tube, and  $\lambda$  is the wave length. The author describes the phenomena by using a single plate called a "thermoacoustic couple". A schematic drawing of a three plate thermoacoustic couple is shown in fig. 2. When the acoustic power is turned on, the heat diffuses through the thermal boundary layer of the gas. As known, the heat moves from the side which supplies the heat energy to the side which absorbs it. More appropriate discussion could be in terms of entropy which flows out of one end of the plates, down along the thermal boundary layer in the gas, and into the other end of the plates. As the ends of the couple are not connected to the external thermal reservoirs the heat flows at the ends are supplied from the plates themselves, which thus gets cooled at the end which supplies the heat flow and heated at the end which absorbs it. In the steady state the return heat flow is diffusive and is driven by the temperature difference. Experiments on the temperature using a U-tube configuration were also conducted by the authors.

Garrett and Hofler (1991) used these results to describe a new refrigerator which uses resonant high amplitude sound in inert gases to pump heat. The thermal contact (phasing) of the various processes of the thermoacoustic cycle is provided by conduction. This natural contact (phasing) allows the entire refrigerator to operate with only one moving part. The experimental setup (fig. 3) is a tube closed at one end and open at the other with a loud speaker fixed at that end. The length of the tube is one quarter wavelength. The loudspeaker at the end sets up an standing wave in the helium filled tube. The

frequency is chosen so that the loudspeaker excites the fundamental resonance of the tube. At the closed end the velocity of the particle is zero and the acoustical pressure variations are maximum. At the loudspeaker end there is an acoustic pressure node and a velocity antinode. The stack of plates is placed near the closed end. The distance between the closed end and the stack is very critical as well as is the distance between the plates of the stack which is called the thermal penetration depth.

The thermal penetration depth represents the distance over which heat will diffuse during a time period which is on the order of an acoustic period. The diffusive heat transport between the gas and the stack is significant within this region. As the fluid oscillates back and forth along the plate it undergoes changes in temperature due to the adiabatic compression and expansion resulting from the pressure variations which accompany the standing sound wave. The compressions and expansions of the gas constitute the sound wave and are adiabatic if they are far from the surface of the plate. The relation between the change in gas pressure due to the sound wave,  $P_1$ , relative to the mean (ambient) pressure  $P_m$ , and the adiabatic temperature change of the gas due to  $T_1$ , to the acoustic pressure change, relative to the mean absolute temperature,  $T_m$  is given as,

$$\frac{T_1}{T_m} = \left( \gamma - \frac{1}{\gamma} \right) \left( \frac{P_1}{P_m} \right) \quad (2)$$

$\gamma$  is the ratio of the specific heats of the gas (5/3 for He). Hofler considered a thermodynamic process as consisting of two reversible

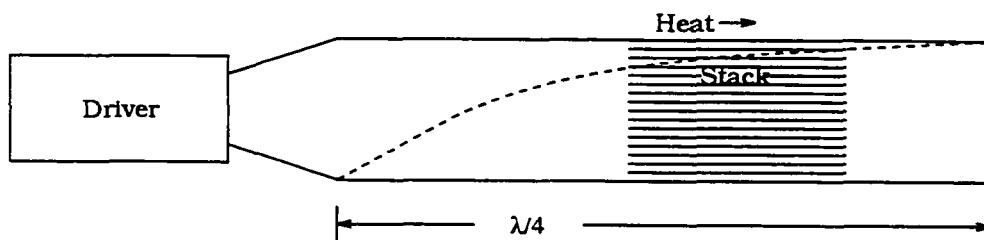


**Fig 3. Schematic diagram of one quarter wavelength, thermoacoustic refrigerator used by Garrett (1991). The dotted line denotes the pressure profile inside the tube.**

adiabatic steps and two irreversible isobaric steps (described in the next chapter).

If there are no external heat loads, then eventually the temperature gradient in the plate approaches the gradient caused by the adiabatic processes in the gas. In the absence of gas viscosity, the critical temperature gradient is a function only of the gas thermophysical properties, the wavelength ( $\lambda$ ), and the mean position of the stack ( $x$ ), within the standing wave field. This temperature gradient is given by (Garrett, 1991),

$$\nabla T_{cr} = 2\pi \frac{(\gamma - 1)}{\lambda} \tan\left(\frac{2\pi x}{\lambda}\right) \quad (3)$$

the ratio between the temperature gradient in the stack ( $\nabla T_m$ ) and the critical gradient,

$$\psi = \frac{\nabla T_m}{\nabla T_{cr}} \quad (4)$$

Assuming the stack is much shorter than the wavelength of the sound, the rate of heat transport or heat pumping power,  $Q_2$  is given by (Garrett, 1991),

$$Q_2 = -\frac{\Pi}{4} \delta_k P_1 u_1 (\psi - 1) \quad (5)$$

Here  $\Pi$  is the stack surface area per unit length and  $u_1$  is the (subscript 1 is the time varying function) particle velocity in the

stack. The work absorbed by the stack of length  $\Delta x$ , in the absence of viscosity is given as (Garrett, 1992), (assuming the heat capacity of the stack is much greater than that of the gas)

$$W_2 = \frac{\Pi}{4} \delta_k \Delta x \frac{(\gamma-1)}{\gamma p_m} 2\pi f (p_1)^2 (\psi-1) \quad (6)$$

In this paper the authors also briefly describe the space thermoacoustic refrigerator, which was first demonstrated in the space shuttle. The description includes the acoustical sub-systems, electrical sub-systems, and refrigerator performance.

Hofler (1988) discusses in detail the design, construction, and calibration of a high intensity acoustic driver apparatus in an acoustic refrigerator with instrumentation for accurate measurements of dynamic pressure, volume velocity, and relative phase. Therefore acoustic power supplied by the driver can be determined from these measurements. These acoustic power measurements will determine the intrinsic acoustic-to-thermal efficiency of the refrigerator.

## **HEAT TRANSFER IN OSCILLATING FLUIDS**

Repin (1985) analytically solves the problem of the effect of a transverse resonant acoustic field on the heat transfer process in a laminar two dimensional channel flow. Repin considers the situation of a tube of infinite length and width  $2d$ . The cross section of the channel is divided into two regions: an inner region, with the

transverse dimension of the order of  $\delta_1$  (acoustic boundary layer), and an outer region with characteristic dimension  $l$ .

It has been described that the outer and inner vortex flows play different roles in the heat transfer process. When the thickness of the thermal boundary layer is much less than that of the acoustic layer, then the inner flows play the decisive part in the heat transfer process. At low acoustic field intensities there is only a slight decrease in the integral heat transfer, however at high intensities the acoustic field has a positive effect. Also the so called "critical acoustic pressure level" is described, i.e., the pressure below which the acoustic field has no effect on the heat transfer process.

It has been emphasized in the paper that the heat transfer process is different for cases of small and large acoustic field amplitudes. Also if a number of conditions are satisfied (*e.g.*, for laminar flow regime when  $Pr \gg 1$ ), a situation may arise where the heat transfer regime changes with distance downstream. In this situation, the heat transfer maximum is displaced from the pressure antinode of the standing wave to the velocity antinode.

Kurzweg has analytically and experimentally dealt, in detail, with the heat transfer between two fluid reservoirs maintained at different temperatures and connected to each other via a capillary bundle when the fluid within the capillaries is oscillated (sinusoidal) axially. Very large effective axial heat conduction rates, exceeding those possible with heat pipes by several orders of magnitude, are found to be achievable (Kurzweg and Zao, 1984). The frequency used was between 2 to 8 Hz and the tidal displacement within the capillaries ranged from 2 to 12.5 cm. The tidal displacements were

determined from the maximum movement of the water from the lower reservoir. The observations made in this regard were that the effective thermal diffusivity is proportional to the square of the tidal displacement and the square root of the oscillation frequency.

The corresponding heat flow between the fluid reservoirs is given by,

$$\dot{Q} = \rho c_p \kappa A_0 \left( \frac{T_h - T_c}{L} \right) \quad (7)$$

$\rho$  is the fluid density,  $c_p$  its specific heat, and  $\kappa$  is thermal diffusivity.  $T_h - T_c$  is the instantaneous temperature difference,  $L$  is tube length and  $A_0$  is total fluid cross sectional area.

The results of the experiments supported the assumption made by the author that in a laminar axial conduction process, formation of very thin boundary layers leads to large radial heat flows which eventually manifest themselves by producing a very large axial heat flux. This means that the radial variation of temperature produce an effective axial transport of heat. Kurzweg (1988) examined the problem of thermal pumping existing in the classical Stokes problem of a sinusoidally oscillating flat plate immersed within a viscous fluid of infinite extent. A constant temperature gradient is superimposed on the fluid parallel to the plate surface and in the direction of plate motion. It is shown that this leads to a large longitudinal heat flux within a relatively narrow boundary layer region next to the plate.

Enhanced conduction heat transfer between two fluid reservoirs maintained at different temperatures was examined

analytically by Kurzweg (1985). He suggested that a thermally conducting fluid confined to an open ended tube with thermally insulating walls and connected to different reservoirs at its ends can be made to conduct heat at rates orders of magnitude greater than by pure conduction, provided the fluid is oscillated sinusoidally in the tube.

Having determined the value of the enhanced thermal diffusivity, he then calculated the heat flow expected between the fluid reservoirs connecting the tubes. The effective axial heat flow per tube was

$$Q = K\pi a^2 \left[ 1 + p(\alpha) \frac{(Pr \Delta z)^2}{16a^2} \right] \frac{(T_H - T_C)}{L} \quad (8)$$

where  $K$  is the fluid thermal conductivity. The conclusion he reached in his paper is, during most of the sinusoidal cycle, the fluid near the wall will have a temperature different from the core. Therefore large quantities of heat will be transferred radially and hence transported axially. The author suggests that this theory may find applications in areas where natural convection is not present or undesirable and also in areas where heat transfer is required without accompanying mass transfer. This shows that the heat transfer in the boundary layer of the thermoacoustic refrigerator plates moves axially but varies radially along the tube. The details of the transport of heat are carried in the next chapter.

Kurzweg (1986) examined the heat flux within an oscillating fluid, in which a constant axial temperature gradient was maintained.

He found that the resultant axial heat flux pulsates at twice the base oscillation frequency and that the time averaged axial heat flux under tuned conditions is orders of magnitude larger than that present in the absence of oscillations. Unlike other convective heat transfer methods, his thermal pumping technique involved no net convective mass transfer and therefore according to him should find considerable application in areas where heat has to be removed at high rates without the accompanying exchange of mass (i.e. cooling of radioactive liquids). This conclusion of the author supports the theory of thermoacoustics in which the heat will be transported from one point to another only by conduction of the fluid particles, without the transfer of mass.

The geometry Kurzweg studied was a tube with counter oscillating slug flows bounded by outer non-conducting walls. The heat transfer process here consists of time dependent transverse conduction coupled to a periodic axial convective transport. The overall effect of this cyclic interactive process is to transport large quantities of heat from the hot to the cold ends of the oscillating fluid slugs. This heat flow increased both with frequency and amplitude.

The enhanced longitudinal heat transfer through an oscillating viscous fluid in an array of parallel plate channels with conducting sidewalls is examined without any restriction on the oscillatory frequency or the side wall conductivity (Kurzweg, 1985). The axial thermal diffusivity was found to be a function of the Womersely number ( $Wo$ ), the fluid Prandtl number and the fluid to wall conductivity.

$$Wo = c\sqrt{\frac{\omega}{\nu}} \quad (9)$$

where  $\omega$  is angular velocity,  $\nu$  is kinematic viscosity, and  $2c$  is the width of fluid layer. The thermal diffusivity reaches maximum (for a fixed frequency) when  $Wo^2 Pr = \pi$ .

An analytical study of forced convection in slow laminar flow in a channel with uniform heat addition and flow oscillations has been performed (Siegel, 1987). The effect of the forced convection (throughflow of fluid) and uniform heat addition is that it will reduce the channel heat transfer coefficient. This conflicting result compared to other studies (without any throughflow of fluid) is because the heat addition along the channel wall produces an increasing fluid temperature along the channel length. The flow oscillations interacting with this positive temperature gradient will induce a heat flow back towards the channel inlet. This will tend to inhibit the heat transfer process and will raise the wall temperature required to transfer away a given amount of heat at the channel wall. The heat transfer behavior is influenced by many parameters such as whether the flow is laminar or turbulent, fully developed or not, the oscillation frequency and the Prandtl number.

Galillin and Khalimov (1985) studied the heat transfer under conditions when the resonance amplitude of the velocity pulsations reaches 160 m-sec and the shock waves radiate from the open end of the tube in which they created the resonant longitudinal oscillations of an air column. The thermal measurements were made by using two sensors which they called the "hot" sensor and the "cold" sensor. In the work with the hot sensor the thermal flux from the inner wall of

the sensor housing was transmitted to the oscillating air stream, heated to a temperature  $T_\infty$  less than the sensor wall temperature  $T_c$  but greater than the wall temperature of the adjacent tube sections. The cold sensor was also a tube section with flanges at the working segment. A tube segment of large diameter was installed coaxially with the first segment. The thermal flux was determined from the change of the heat content of water passed through the annular gap. The tube sections adjacent to the sensor were heated. The researchers made some provisions in the sensors for the introduction of velocity and pressure sensors and the resistance thermometer. The temperature at the sensor wall was measured with the help of thermocouples.

The heat transfer coefficient was calculated as,

$$\alpha = \frac{q_f}{T_c - T_\infty (1 + \psi \frac{\gamma - 1}{2} \bar{u}^2)} \quad (10)$$

where  $q_f$  is the thermal flux density;  $T_c$ ,  $T_\infty$  are the thermodynamic temperatures of the sensor wall and the air;  $\psi = 0.85$ ;  $\bar{u} = u/a$  is the dimensionless half amplitude of the velocity pulsations ( $a$  is the speed of sound in the undisturbed medium). The readings they had taken from the oscillograms of the velocity and pressure pulsations at the linear resonance  $f_1 = a/4L$  and second linear resonance  $f_2 = 3a/4L$  show that the shock waves radiate from the open end of the tube, where  $L$  is the length of the tube and  $f_1$  is the fundamental frequency. At the open end with a tube length of  $L = 3.5$  m, the velocity pulsation was maximum. The velocity pulsation was 155 m-sec.

According to the researchers the dependence of the Nu number on the frequency was not uniform. There were two heat transfer intensity maxima, one corresponds to the case  $f_1$  and the other to  $f_2$ . The resonance frequencies of the numbers Nu and  $\bar{U}$  coincide. An increase in the tube length was accompanied by a reduction of Nu number. The results varied with the position of the sensors. Again the reduction of the tube length leads to an increase of the velocity half amplitude and consequently to an increase of the heat transfer coefficient. The frequency of the large amplitude (30-150 m-sec) oscillations had no direct influence on the heat transfer.

They conducted several experiments with different tube lengths and frequencies which they related to the quasisteady theory. The results were in good agreement with the theory.

Joshi *et al.* (1983) conducted experiments to determine the effective diffusivity for axial transport through a tube of a contaminated gas in oscillatory flow. The results demonstrated the rapid fall in the rate of axial dispersion as frequency increases at constant velocity amplitude.

Nonlinear coupling between two oscillating modes can generate abundant nonlinear phenomena, quasiperiodicity, frequency locking, and quenching phenomena (Yazaki *et al.*, 1990) when a spontaneous acoustic oscillation of a gas column induced by temperature gradient is periodically perturbed by an external force.

Numerical simulation was conducted on the heat transfer mechanism involved in the sinusoidal motion of a fluid by Ozawa (1991). The effective thermal diffusivity in the axial direction was formulated based on the lumped parameter heat transfer model. The

enhanced heat transfer is due to the lateral diffusion of heat, accumulated capacity of heat in a region of depth of penetration formed near the wall, and convective motion forced by the oscillation.

Numerical computations of heat and mass transfer were performed on the effect of an oscillatory flow (acoustic field) with steady and time varying velocity component (Ha, 1993,a and b). The increase in the Nusselt number is found to be more significant for larger acoustic velocities. Enhanced mass transfer in a hydraulically fully developed flow within a tube for steady, pulsating and oscillating flow was investigated by Grassman (1978).

An experimental investigation was done on the heat transfer between the gas and the cylinder wall when pressure is very non-sinusoidal (Yagaya, 1991). An advanced complex Nusselt number model is introduced in this paper which helps describe the actual heat transfer rate in a gas where pressure and temperature variations of the gas are non-sinusoidal.

## **CHAPTER 3**

# **ANALYSIS**

### **INTRODUCTION**

For a better understanding of the working of acoustic refrigerators, it is important to understand the effects of a sinusoidal wave in a tube with an ideal gas (ideal gas is taken to assume that the perfect conditions exist in the tube). What happens inside when the gas is driven has been studied in detail by Merkli and Thomann (1975). Therefore a tube like this is called a "Merkli and Thomann tube". The heating of the closed end and the cooling in the region of maximum velocity is reported.

### **THEORY**

To analyze how this temperature gradient is created, first an analysis of the boundary layer of the tube wall without the stack will be done and the analysis with the stack will be considered later. Most of the concepts of the tube wall boundary layer will suffice to the boundary layer of the stack plates.

It is essential to understand that the velocity is zero near the end of the tube (closed end) and is equal to the velocity amplitude at the driver end. The velocity throughout the length of the tube changes parabolically with the maximum velocity (velocity antinode) almost at the center of the tube. The pressure variation across the tube is uniform and along the length varies with maximum values (pressure antinode) at the closed and the driver ends. At the center of the tube, the pressure is zero (pressure node). In the ideal acoustic case where viscosity and thermal conductivity are assumed negligible ( $\mu=0$ ,  $K=0$ ), no net energy flux exists in the tube as the phase between velocity and pressure equals  $\pi/2$ . This means that the correction arising from the non-vanishing viscosity and the heat conductivity are the real and only sources of thermal effects from acoustic oscillations.

Since velocity and pressure are in phase (therefore velocity and temperature are in phase), a flow directed from the velocity maxima towards the end of the tube has a temperature above equilibrium temperature (atmospheric) while a flow away from the ends (nodes) is below atmospheric temperature, which leads to a net enthalpy flux towards the ends. According to the calculations done by Merkli and Thomann an enthalpy flux exists in the tube, even though the sound wave is adiabatic in nature. But due to the pressure oscillations an amount of heat will be carried in the boundary layer due to the high viscous dissipation. In the frequency range where pressure is uniform across the tube cross section and for high Reynolds numbers, a thin boundary layer forms at the wall where penetration depths (discussed later) are formed. The enthalpy flux which varies with length

corresponds to the heat exchanged with the tube wall. Since the heat flows from the point of maximum velocity towards the point of lower velocity, there is cooling at the center and heating at the ends. Most of this phenomena occurs in the boundary layer, if the Prandtl number of the fluid is low ( $Pr \ll 1$ ).

In such a case where the gas is driven sinusoidally, the heat transfer between the gas and the solid boundary is the most important effect. Two important quantities, "thermal penetration depth" ( $\delta_k$ ) and "viscous penetration depth" ( $\delta_v$ ) are to be defined, as in this small distance from the wall, the heat transfer phenomena are active.  $\delta_k$  has been defined as the distance from the wall in which heat can diffuse through the fluid during the time  $1/\omega$ .  $\delta_k$  for air at 1000 Hz is 0.01 (Swift, 1988).  $\delta_v$  is defined as the distance from the wall in which momentum diffuses through the fluid in time  $1/\omega$ . Both  $\delta_k$  and  $\delta_v$  are assumed to be very small compared to wavelength and the diameter of the tube ( $\lambda \gg d \gg \delta$ ). Since the diameter of the tube is much smaller than the wavelength, the pressure distribution across the width at a given instant in time is approximately uniform. Therefore pressure is independent of direction 'y' (direction 'x' taken along the tube axis and 'y' is transverse). The two dimensional cartesian coordinate system in the complete refrigeration system with plates (stack) which will be used through out this analysis is as shown in fig. 4.

## ANALYSIS

To explain how the temperature is related to the pressure, we will assume that an expansion to the first order pressure amplitude

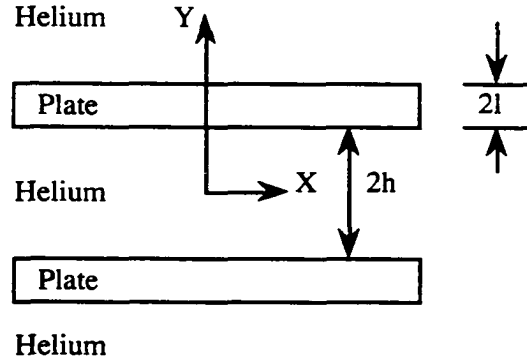


Fig. 4. An expanded view of co-ordinate system used for the analysis with plate and spacing thicknesses.

suffices for all thermodynamic and acoustic variables (temperature, density, pressure, velocity, entropy) and will also include the complex notation for time oscillatory quantities (as shown below). This notation for pressure, density, velocity, temperature in the fluid, temperature in the solid ( $T_f$ ), and entropy of the wave can be written as,

$$\begin{aligned}
 P &= P_m + P_1 e^{i\omega t} \\
 \rho &= \rho_m + \rho_1 e^{i\omega t} \\
 u &= u_1 e^{i\omega t} \\
 T &= T_m + T_1 e^{i\omega t} \\
 T_f &= T_m + T_{f1} e^{i\omega t} \\
 s &= s_m + s_1 e^{i\omega t}
 \end{aligned}
 \tag{11}$$

with  $P_1$  a function of position,  $e^{i\omega t}$  showing the time dependence. The mean values (subscript m in this case) will be real, but the small amplitudes (subscript 1) will be complex, reflecting time phasing of the oscillating quantities. The real part of the complex solution represents an actual, physical solution. The subscript f represents the film or plate of the stack.

Since the sound wave without the stack plates is adiabatic, the oscillating temperature  $T_1$  is related to the pressure  $P_1$  by,

$$T_1 = \left(\frac{\partial T}{\partial P}\right) P_1 = -\frac{1}{\rho_m^2} \left(\frac{\partial \rho}{\partial s}\right) P_1 = \frac{T_m \beta}{\rho_m c_p} P_1 \quad (12)$$

where  $s$  is the entropy per unit mass and  $\beta = -(\partial \rho / \partial T) / \rho_m$  is the ordinary thermal expansion coefficient. Since  $T_m \beta / \rho_m c_p$  is positive and real,  $T_1$  and  $P_1$  are in phase in an ordinary sound wave.

To explain the heat transfer from the wall, consider a small parcel of gas which is oscillating in the  $x$  direction at about one penetration depth from the wall in the  $y$  direction. Due to the thermal resistance of this gas parcel which also has some heat capacity, heat will be conducted through the parcel. The pressure variation is needed to produce the temperature difference, and the velocity is needed to transport the gas parcel. All oscillations have temperature changes associated with them due to the compressions and expansions. Therefore when oscillations start, heat will be exchanged between the gas and the container (tube). At this point it is appropriate to introduce the concept of "thermoacoustic streaming". Due to this streaming, the axial temperature gradient is

found to carry heat much more effectively than the Fourier conduction caused by the same gradient, a fact well proven experimentally and confirmed theoretically by Rott (1975). It is reported that there is maximum cooling at the velocity antinode and maximum heating at the pressure antinode.

To increase the surface area, a stack is placed in the tube, so that the thermal penetration depth on each plate increases the amount of heat carried from one point to another. The cooling and heating at the ends of the plates are central to the thermodynamic phenomena which are the essence of this thesis. Effects at the ends can be emphasized and the phenomena simplified by making the stack of plates short. The apparatus can be further simplified by reducing the number of plates. Indeed, all the phenomena to be described below can be observed in a single plate which is called a "thermoacoustic couple" (Wheatley, 1983). Fig. 2 shows the single couple and all the heat transfer process associated with it will be investigated, i.e. as to how the plate (stack plate) which is the central part of our argument, transmits heat from one point to another.

The heat conduction equation in fluids which is given later has terms containing temperature and velocity. Since the pressure has a major effect on the conduction in an acoustic system, an equation relating temperature and pressure is essential for better understanding of the analysis. From the thermodynamic relations given later, the time dependent temperature can be related to entropy and in turn entropy can be related to the required pressure and temperature. This gives us the final equation derived subsequently which relates the heat conduction terms, pressure and

velocity. The entropy formulation of the equations is done here as the resonance shock wave is found to have the entropy changes associated to it. The change of entropy is found to govern various thermodynamic properties in an ordinary wave or a shock wave. However, entropy in this case works as a carrier of heat and the energy from one point to another. Also from the statements given above, it can be considered that the heat flow in the gas is due to the hydrodynamic transport of entropy and carried by the oscillatory velocity. Therefore the entropy is used only initially during the analysis, but does not appear in the final equations which governs the heat flow.

In thermoacoustic engines, the primary part of importance is the stack and the secondary is the gas. Therefore the contact between gas and the stack plate has to be understood clearly. When the acoustic power is applied by the driver, (loudspeaker or piston moving sinusoidally) it causes an average flow of entropy from one end to the other end of the plate along the thermal boundary layer in the gas. As these ends of the plate are not connected to any external source the heat is supplied from the plate itself. Therefore the end which supplies the heat gets cooled and the other end which absorbs gets heated. The entropy can be expressed in terms of pressure and temperature by the thermodynamic relation

$$ds = \frac{c_p}{T}dT - \frac{\beta}{\rho}dP \quad (13)$$

therefore, for small oscillations :

$$s_1 = \frac{c_p}{T_m} T_1 - \frac{\beta}{\rho_m} P_1 \quad (14)$$

The conduction equation which can be used to find the temperature in the fluid is called the energy equation (White, 1986). It is valid for a Newtonian fluid under very general conditions of unsteady, compressible, viscous, heat-conducting flow, except that it neglects radiation heat transfer and internal heat generation. Starting from the fundamental Fourier's law,

$$q = -K \nabla T \quad (15)$$

the equation for conduction in 3 dimensional Cartesian coordinates in fluids is developed, which in tensor notation is,

$$\rho c_v \frac{dT}{dt} = \nabla \cdot (K \nabla T) + \Phi \quad (16)$$

where if K is constant (also  $C_p$ ,  $C_v$ ,  $\mu$ ,  $\rho$  are constant and viscous dissipation is always positive),

$$\nabla^2 T = \frac{\partial^2 T}{\partial x^2} + \frac{\partial^2 T}{\partial y^2} + \frac{\partial^2 T}{\partial z^2}$$

$$\Phi = \mu \left[ 2 \left( \frac{\partial u}{\partial x} \right)^2 + 2 \left( \frac{\partial v}{\partial y} \right)^2 + 2 \left( \frac{\partial w}{\partial z} \right)^2 + \left( \frac{\partial v}{\partial x} + \frac{\partial u}{\partial y} \right)^2 + \left( \frac{\partial w}{\partial y} + \frac{\partial v}{\partial z} \right)^2 + \left( \frac{\partial u}{\partial z} + \frac{\partial w}{\partial x} \right)^2 \right]$$

The above equation is now written in the form containing entropy because the heat transport in a sound wave is found to be governed by the entropy changes associated with the wave and also

the reasons explained earlier, therefore from Landau and Lifshitz, 1987,

$$\rho c_v \frac{\partial T}{\partial t} = \rho T \left( \frac{\partial s}{\partial t} + \mathbf{V} \cdot \nabla s \right) \quad (17)$$

where  $\mathbf{V}$  represents  $u, v$ , and  $w$  (velocity components).

Now substituting eqn. (17) into eqn. (16) and neglecting the thermal conduction along  $x$ , the velocity advection terms can be neglected, and after substituting the relations (11), we have,

$$\rho_m T_m \left( i \omega s_1 + u_1 \frac{d s_m}{dx} \right) = K \frac{d^2 T_1}{dy^2} \quad (18)$$

by substituting eqn. (13) and (14) in the above equation, we have the final differential governing equation as,

$$\rho_m c_p \left( i \omega T_1 + u_1 \frac{d T_m}{dx} \right) - i \omega T_m \beta P_1 = K \frac{d^2 T_1}{dy^2} \quad (19)$$

The boundary conditions are,

$$T_1(h) = T_{fl}(l) = T_{b1}$$

and

$$K \left( \frac{\partial T_1}{\partial y} \right) \Big|_h = -K_f \left( \frac{\partial T_{fl}}{\partial y} \right) \Big|_l \quad (20)$$

In the above equations  $2h$  is the thickness of the spacing between two plates and  $2l$  is the thickness of the plate itself.  $T_b$  is the temperature amplitude at the boundary  $y = h$ , which can be calculated from its relation with  $T_f$  given in detail (Swift, 1988).  $T_{f1}$  is the first order temperature in the solid or film (plate).  $K_f$  is the thermal conductivity of the film.

To calculate the acoustic velocity,  $u$ , the two dimensional Navier Stokes equation in the  $x$  direction is used, which is,

$$\rho \left( \frac{\partial u}{\partial t} \right) = - \frac{\partial p}{\partial x} + \frac{\partial}{\partial y} \left[ \mu \left( \frac{\partial u}{\partial y} + \frac{\partial v}{\partial x} \right) \right] + \frac{\partial}{\partial x} \left[ \mu \left( \frac{\partial u}{\partial x} - \frac{2}{3} \left( \frac{\partial u}{\partial x} + \frac{\partial v}{\partial y} \right) \right) \right] \quad (21)$$

using the relations (11), the above equation can be written as,

$$i\omega\rho_m u_1 = - \frac{\partial P_1}{\partial x} + \mu \frac{\partial^2 u_1}{\partial y^2} + \mu \frac{\partial^2 v_1}{\partial x^2} + 2\mu \frac{\partial^2 u_1}{\partial x^2} + \frac{2}{3}\mu \frac{\partial^2 u_1}{\partial x^2} - \frac{2}{3}\mu \frac{\partial^2 v_1}{\partial x \partial y} \quad (22)$$

Since the viscous penetration depth is much smaller than the wavelength ( $\delta_v \ll \lambda$ ) and also  $\partial/\partial x$  is of the order of  $1/\lambda$  and  $\partial/\partial y$  is of the order of  $1/\delta_v$ , all other terms compared to  $\partial^2 u_1/\partial y^2$  may be neglected and the pressure term appears as it is constantly changing along  $x$ . Therefore the above equation can be written as,

$$i\omega\rho_m u_1 = - \frac{\partial P_1}{\partial x} + \mu \frac{\partial^2 u_1}{\partial y^2} \quad (23)$$

The boundary conditions are,

$$u_1(h) = u_1(-h) = 0 \quad (24)$$

The solution is (Appendix B),

$$u_1 = \frac{1}{i\omega\rho_m} \frac{dP_1}{dx} \left[ \frac{2(1 - e^{-2gh})}{eg(1 - e^{-4gh})} \cosh(gy) - 1 \right] \quad (25)$$

where  $g = \sqrt{i\omega/\nu}$ .

Since  $u_1$  and  $T_1$  are calculated, they can be used to calculate pressure amplitude ( $P_1$ ) from the wave equation which can be derived from the continuity equation which in 3 dimensions is,

$$\frac{\partial \rho}{\partial t} + \frac{\partial}{\partial x}(\rho u) + \frac{\partial}{\partial y}(\rho v) + \frac{\partial}{\partial z}(\rho w) = 0 \quad (26)$$

by substituting the relations (11) in 2 dimensions, the  $v_1$  term vanishes as it is zero at both the boundaries of plate and fluid, therefore we get,

$$i\omega\rho_1 + \frac{\partial}{\partial x}(\rho_m u_1) = 0 \quad (27)$$

using the equation of state (Swift, 1988) to express  $\rho_1$  in terms of  $T_1$  and  $P_1$ ,

$$\rho_1 = -\rho_m \beta T_1 + \left(\frac{\gamma}{a^2}\right) P_1 \quad (28)$$

using eqn. (23) to substitute  $\rho_m u_1$  and eqn. (28) to substitute  $\rho_1$  in eqn. (27), we get,

$$\omega^2 \rho_m \beta T_1 - \omega^2 \frac{\gamma}{a^2} P_1 - \frac{\partial^2 P_1}{\partial x^2} + \frac{d}{dx} \left( \mu \frac{\partial^2 u_1}{\partial y^2} \right) = 0 \quad (29)$$

Now substitute  $u_1$  and  $T_1$  calculated from the eqns. (25) and (19) and integrate with respect to  $y$  from 0 to  $h$ . This will give the relation for  $P_1$ . The integrated equation is called the "wave equation".

The solution for the above equation is complex and involves various relations from heat transfer, acoustics and fluid mechanics. This complex solution for similar equations as above is done by Swift (1988). The solution is for the energy flux (H) and work flux or acoustic power required to drive such a system.

The energy flux is:

$$\begin{aligned} \dot{H} = & -\frac{1}{4}\pi\delta_k \frac{T_m \beta P_1^s u_1^s}{(1+\varepsilon_s)(1+Pr)(1-\delta_v/h + \delta_v^2/h^2)} \\ & \times \left[ \frac{\psi(1 + \sqrt{Pr} + Pr + Pr\varepsilon_s)}{1 + \sqrt{Pr}} - \left(1 + \sqrt{Pr} - \frac{\delta_v}{h}\right) \right] \\ & - \pi(hk + lk_s) \frac{dT_m}{dx} \end{aligned} \quad (30)$$

and the acoustic power is:

$$\begin{aligned} \dot{W} = & \frac{1}{4}\pi\delta_k \Delta x \frac{(\gamma-1)\omega(P_1^s)^2}{\rho_m a^2(1+\varepsilon_s)} \\ & \times \left( \frac{\psi}{(1 + \sqrt{Pr})(1 - \delta_v/h + \delta_v^2/2h^2)} - 1 \right) \\ & - \frac{1}{4}\pi\delta_v \Delta x \frac{\omega \rho_m (u_1^s)^2}{1 - \delta_v/h + \delta_v^2/2h^2} \end{aligned} \quad (31)$$

In the above equations we have,

$\Pi$  = perimeter

$\beta$  = thermal expansion coefficient

$P_1$  = first order acoustic pressure

$u_1$  = first order acoustic velocity in x direction

$\varepsilon_s$  = plate thermal heat capacity

$Pr$  = Prandtl number

$\Psi$  = normalized temperature gradient

$k$  = thermal conductivity of the fluid

$k_s$  = thermal conductivity of the solid or plate

$\Delta x$  = length of the plate

$g$  = Specific heat ratio

$a$  = Speed of sound in gas

where the superscript s denotes the standing wave.

A FORTRAN program (Appendix A) is written following the above equations to understand how the heat flux and the acoustic power varies with different frequencies and pressure amplitudes and the results are shown in graphical form. In the program helium is used as the fluid, and the stack is a long Kapton (plastic) sheet. Kapton was selected as it has low thermal conductivity and is also easy to roll. Equations 30 and 31 are used for the final analysis of the energy flux and the acoustic power. The equation for the coefficient of performance (COP) ratio is (Swift, 1988):

$$\frac{cop}{cop \text{ (carnot)}} = \frac{\dot{H} \cdot \Delta T}{\dot{W} \cdot T_m} \quad (32)$$

where  $\Delta T$  is the temperature difference across the stack, which is initially an assumed value.

The selection of the proper frequency and pressure for maximum efficiency with minimum acoustic work can be made from the numerical calculations shown here in the form of plots. These graphs are plotted by keeping the thermophysical properties constant for a given set of dimensions of the apparatus.

The graphs on the subsequent pages show the variation of energy flux, acoustic power and the coefficient of performance (cop) when the frequency is varied with pressure remaining constant (Figs. 5, 6 and 7). Note that the length of the device must be varied with frequency in order that the standing wave conditions are met. In figs. 5 and 6, the given range of frequency is selected because the energy flux beyond this range decreases and the acoustic work increases. From the numerical data it was found that the optimum frequency for the given radius of the apparatus is 530 Hz, where the energy flux is 8.32 W and the required acoustic work is 6.87 W. The COP at this frequency was found to be 1.21. Similarly, if pressure is varied with frequency remaining constant, the changes are shown in figs. 8, 9 and 10. The optimum acoustic pressure is 0.3 bar. The cop after this acoustic pressure remains almost constant (fig. 10). Fig. 11 shows the variation of pressure with velocity when the fluid is excited at resonance. The location of the stack is given by fig. 11, which gives an estimate of the choice of pressure and the associated velocity at any particular location. It is a clear indication that the velocity and pressure vary inversely. Therefore the optimum choice of pressure or velocity is essential, so that neither has zero value. Figs. 12 and 13

give the variation of energy flux and acoustic work with the radius of the tube. As can be seen both the energy flux and the work are almost directly proportional to the square of the tube radius. If the radius is varied the total area of the stack varies thereby increasing the effective area on which heat transfer is active.

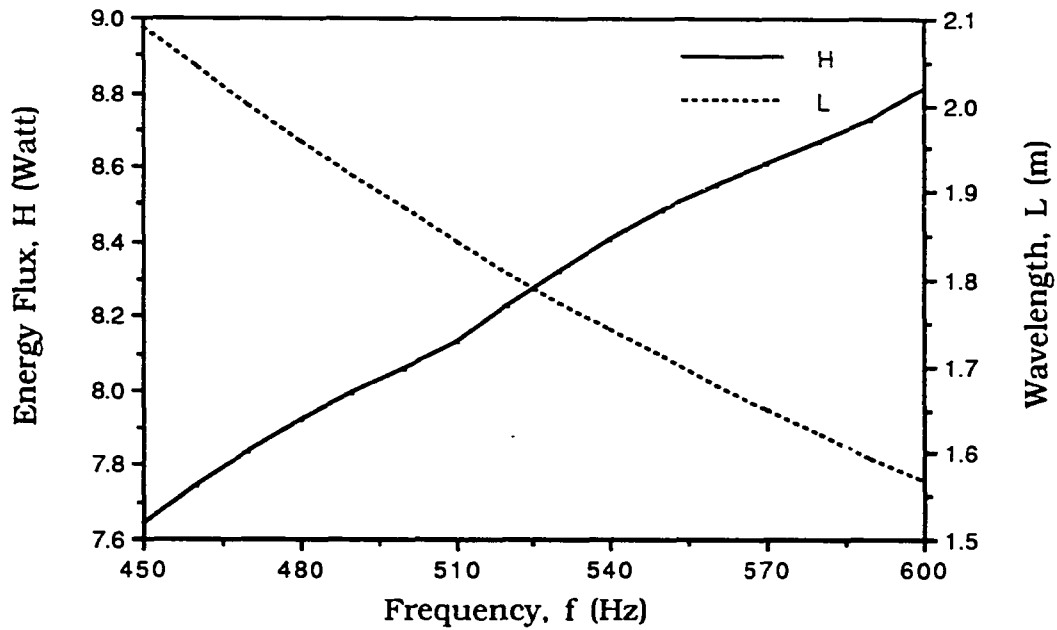


Fig. 5. This plot shows the variation of energy flux,  $H$  (Watt), and wavelength,  $\lambda$  (m) (tube length is  $\lambda/2$ ) with frequency,  $f$  (Hz), at mean temperature,  $T_m = 255$  K; mean pressure,  $P_m = 10$  bar; Specific heat ratio,  $\gamma = 1.67$ ; sound speed,  $a = 940$ ; density of gas,  $\rho_m = 1.9$  kg/m<sup>3</sup>; specific heat at constant pressure,  $C_p = 5.2$  J/g.K; Prandtl number,  $Pr = 0.68$ ; Thermal conductivity of gas,  $K = 0.0013$  W/cm.K; Thermal conductivity of plate or film,  $K_f = 0.0016$  W/cm.K; density of film,  $\rho_f = 0.0014$  kg/cm<sup>3</sup>; specific heat of film,  $c_f = 1.1$  J/g.K.

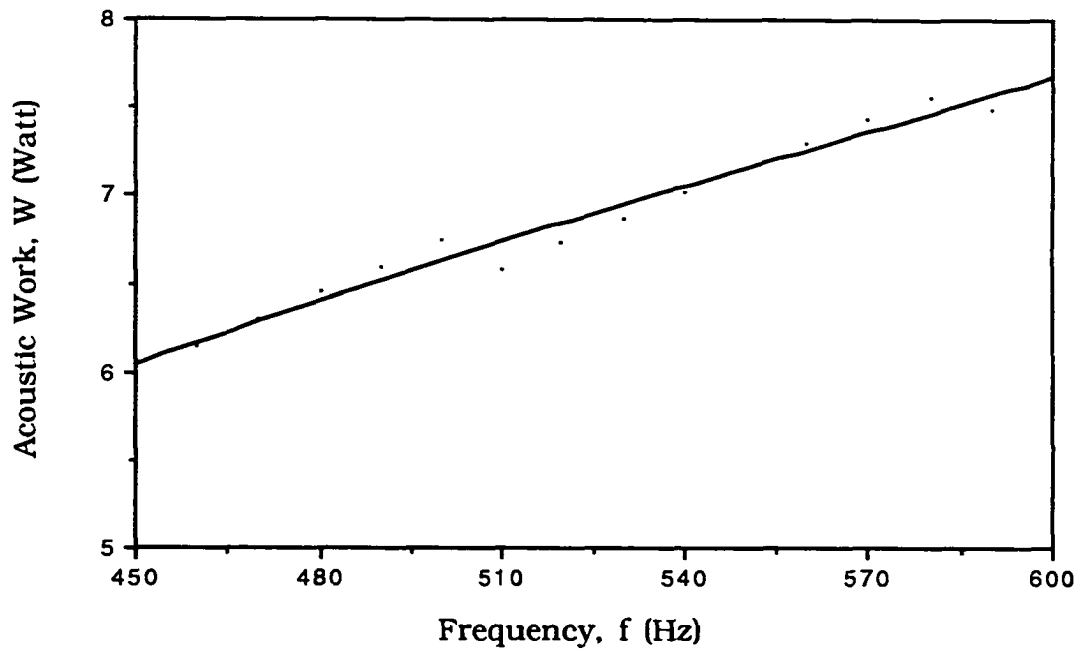


Fig. 6. This plot shows the variation of acoustic power,  $W$  (Watt), with frequency,  $f$  (Hz), at the parameters given in fig. 5.

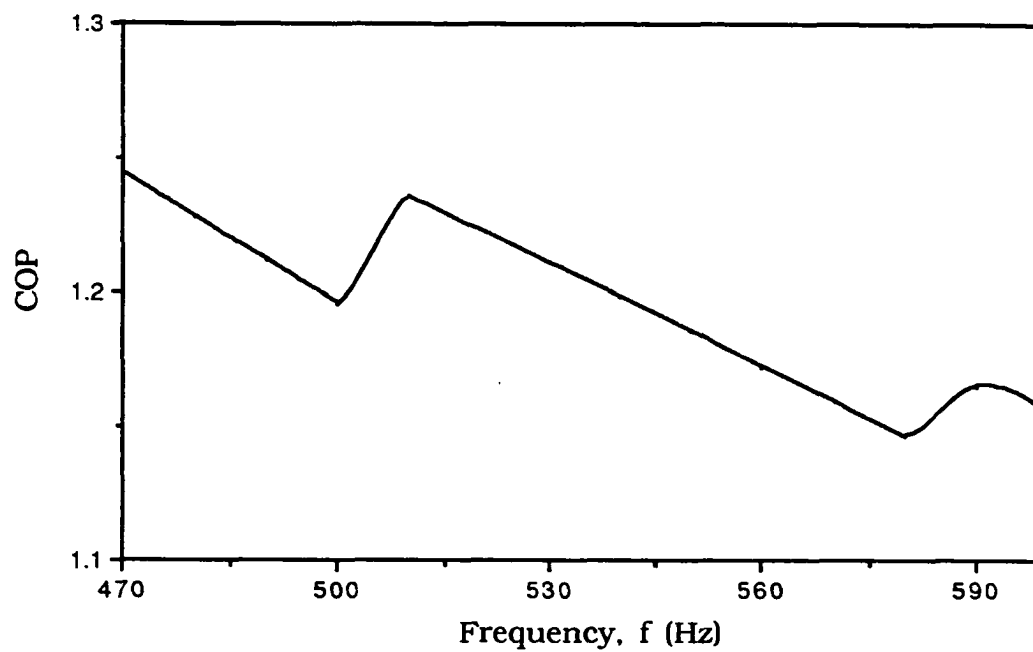


Fig. 7. This plot shows the COP with frequency,  $f$  (Hz), at the parameters given in fig. 5.

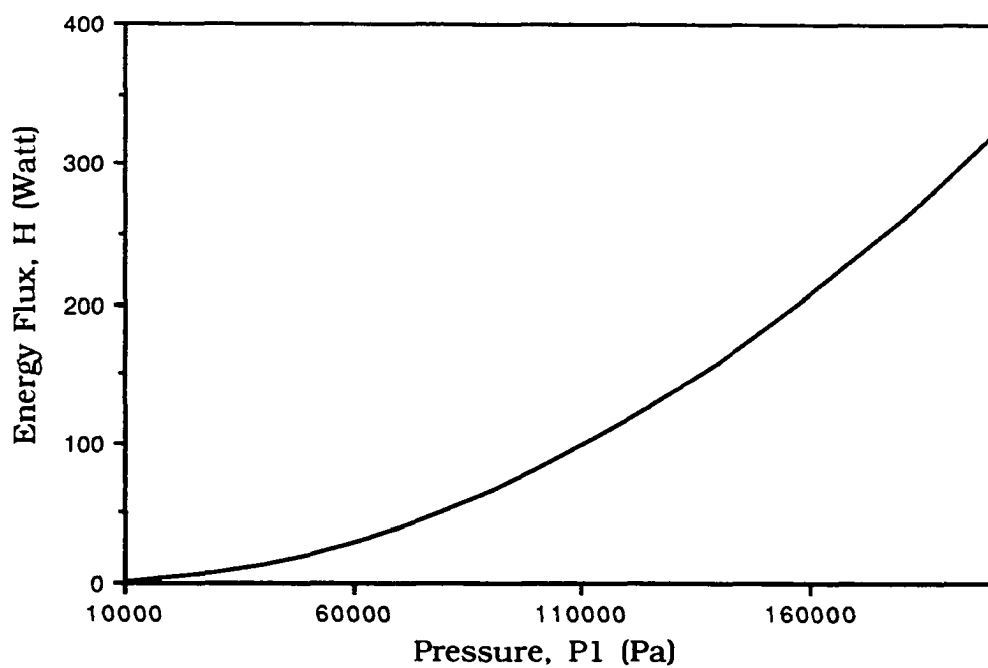


Fig. 8. This plot shows the variation of energy flux,  $H$  (Watt), with pressure amplitude,  $P_1$  (Pascal), at the parameters given in fig. 5.

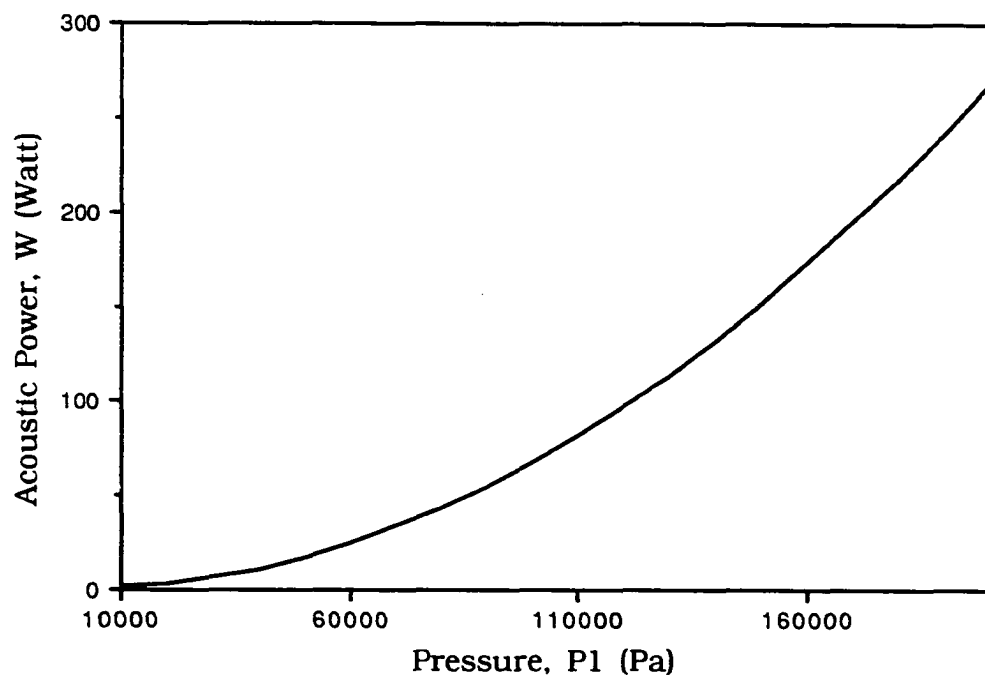


Fig. 9. This plot shows the variation of acoustic power,  $W$  (Watt), with pressure amplitude,  $P_1$  (Pascal), at the parameters given in fig. 5.

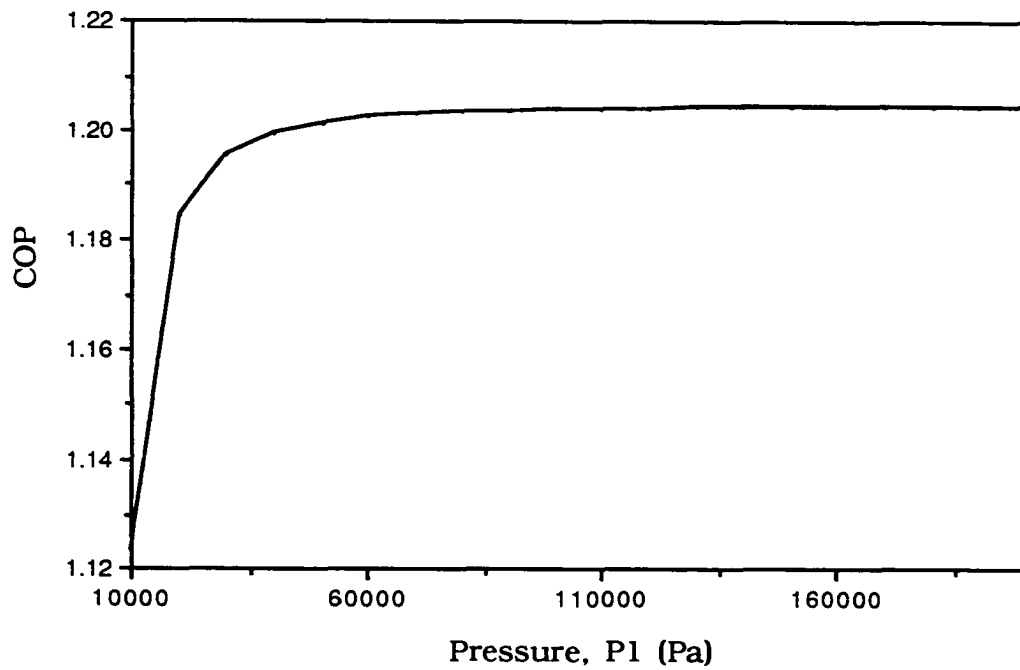


Fig. 10. This plot shows the variation of COP with pressure amplitude,  $P_1$  (Pascal), at the parameters given in fig. 5.

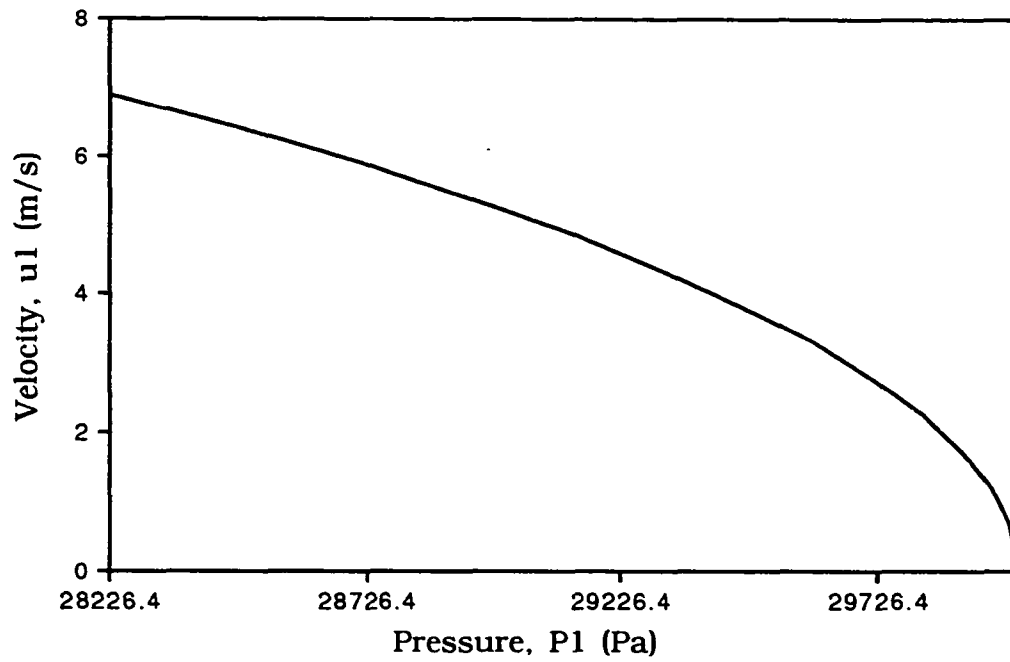


Fig. 11. This plot shows the variation of velocity,  $u_1$ , with pressure  $P_1$  (Pascal), at the parameters given in fig. 5.

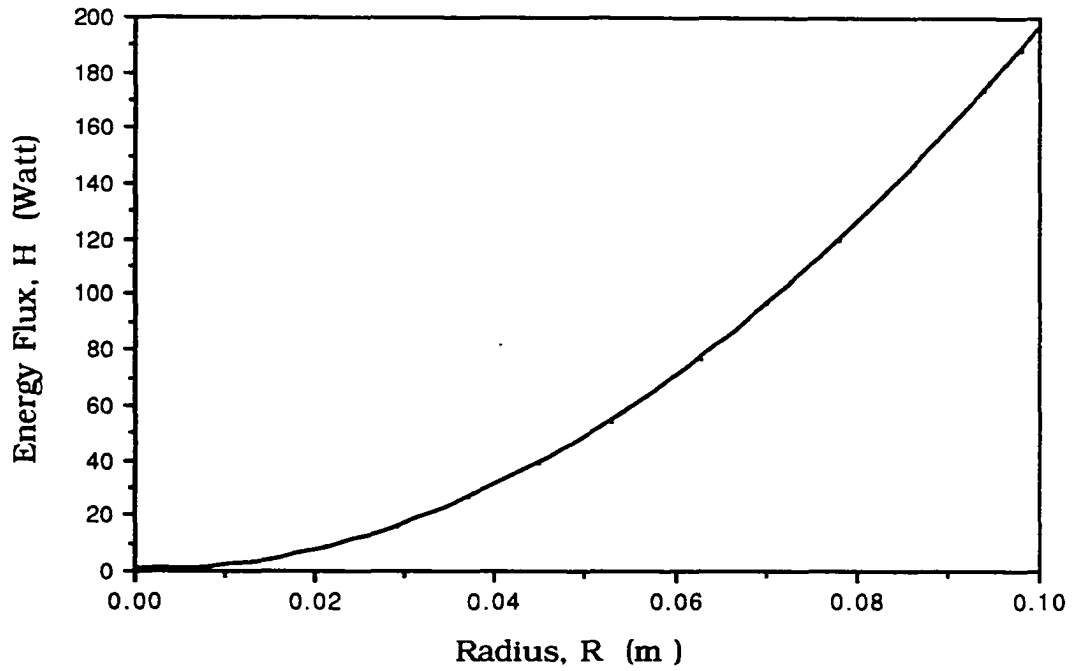


Fig. 12. This plot shows the variation of energy flux,  $H$  (watt), with the tube radius,  $R$  (m), ( $H \propto R^2$ ), at the parameters given in fig.5.

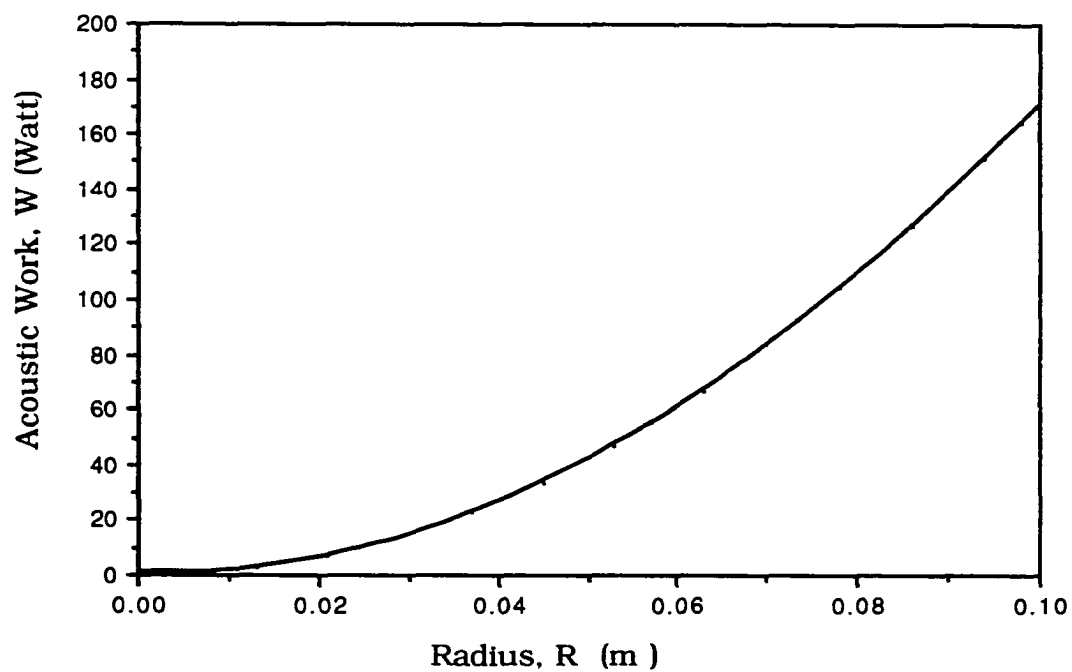
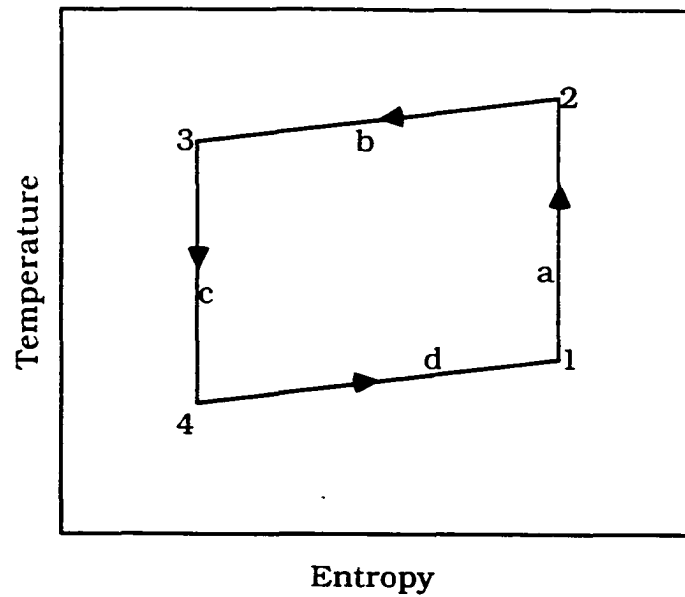


Fig. 13. This plot shows the variation of acoustic work,  $W$  (watt), with tube radius,  $R$  (m), ( $W \propto R^2$ ), at the parameters given in fig. 5.

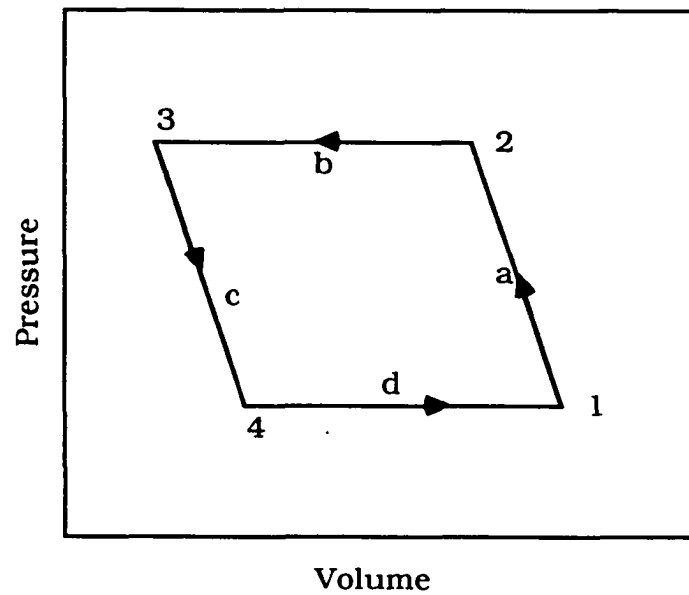
## PHYSICAL DESCRIPTION

As the loudspeaker is switched on, it sets up the standing wave within the gas filled tube. The frequency is chosen so that the loudspeaker excites the fundamental resonance of the tube. Considering a gas parcel undergoing the sinusoidal oscillations, the thermodynamic cycle of oscillations of the gas parcel can be considered as consisting of two reversible adiabatic steps and two irreversible isobaric constant pressure steps as shown in fig. 14. Assuming the plate temperature as  $T_m$  and a temperature gradient  $\Delta T$  referenced to the mean position,  $x=0$ .  $x_1$  is measured from  $x=0$  to the corner of the stack. Therefore the gas parcel at the left most position is  $T_m - x_1 \Delta T$  and at the right most position is  $T_m + x_1 \Delta T$ . In the first step of the cycle, the fluid is transported along the plate by distance  $2x_1$  and is heated by adiabatic compression (process a in fig. 14) from  $T_m - x_1 \Delta T$  to  $T_m - x_1 \Delta T + 2T_1$ .

Here the work in the form of sound is done on the parcel and it is now a temperature higher than the plate temperature. Now the warmer parcel transfers some heat to the plate by thermal conduction between the gas and the plate at constant pressure (process b in fig. 14) reducing its temperature to  $T_m + x_1 \Delta T$ . In the third step, it moves back a distance  $-x_1$  and is cooled by adiabatic expansion to the temperature (process c in fig. 14)  $T_m + x_1 - 2T_1$ . This temperature is lower than the plate temperature, therefore at this step it absorbs some heat from the plate, raising its temperature to its original value  $T_m + x_1 \Delta T$  (process d in fig. 14). The net effect of this process is that the system has completed a cycle and an amount



(A)



(B)

Fig. 14 Thermodynamic cycles with state points and process lines. (A) shows the cycle with entropy and temperature and (B) shows the pressure and volume changes (Wheatley *et al.*, 1986).

of heat has been transported up a temperature gradient by work done in the form of sound. All along the plate a similar situation occurs, but now the gas parcel gives away some heat to its neighboring parcel, thereby transferring heat from one end to another end of the plate. If we place heat exchangers at the ends of the plate, heat will be transferred from one exchanger to another.

At the conditions of uniform temperature, it is advantageous to place the stack in the center of the tube, since the viscous and thermal losses are too high at the ends of the tube. If the temperature is not uniform, i.e., if we allow the engine to develop a negative temperature gradient (hot temperature nearest the pressure antinode), not only the temperature difference and the heat conduction across the boundary layer are reduced and but also the viscous and thermal losses are reduced. Now we can place the stack near the closed end of the tube (pressure antinode) since the temperature span of the engine has increased and also the temperature gradient at the pressure antinode is larger.

The above stack position has problems associated with it. Since the cold end is towards the driver end, there is more heat load on this end. This is due to the heat conducted from the driver to the cold end of the stack. This heat conduction phenomena is due to the acoustically-driven convective flows called "acoustic streaming" (Hofler, 1986).

The above problem can be rectified by driving the system from the opposite end, i.e., by placing the driver near the hot end of the stack. But we cannot simply place the driver at the other end, since this is a velocity antinode. This hurdle can be overcome by increasing

the length of the tube from a quarter wavelength ( $\lambda/4$ ) to half wavelength ( $\lambda/2$ ). Now the driver is at the pressure antinode and therefore the stack can be placed at this end as shown in fig. 15.

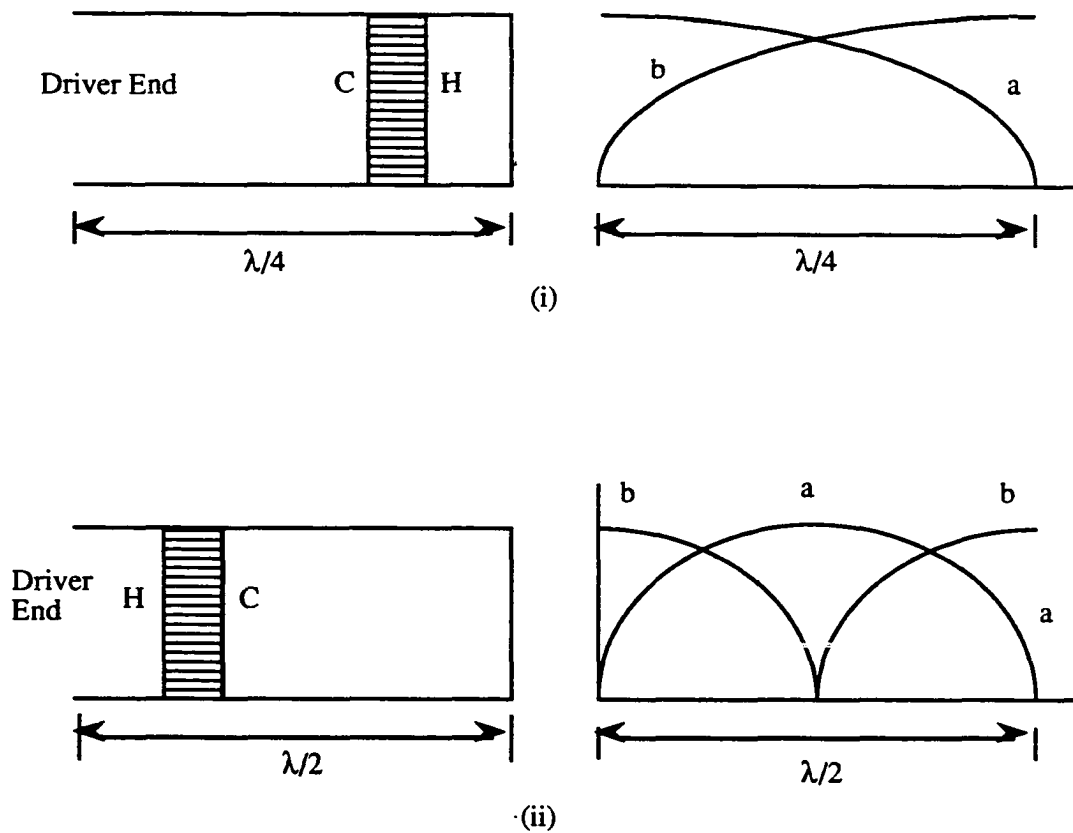


Fig. 15. Developed model of the refrigerator. (i) is the tube of  $\lambda/4$  length with stack and the cold (C) and hot (H) sides. (ii) is the tube with  $\lambda/2$  length. "a" shows the velocity profile and "b" shows the pressure profile.

## **CHAPTER 4**

# **EXPERIMENTAL APPARATUS AND DESIGN**

### **INTRODUCTION**

In this section, the design procedure and the design of the various components will be discussed. The refrigeration apparatus discussed below is the hardware implementation of the theoretical aspects investigated in detail by Hofler and Rott. The design and construction is a very complex and time consuming part of the present study, since it involves very precise dimensions, accurate instrumentation and application of acoustic principles. The theoretical aspects of this design were very briefly discussed by Hofler (1986).

The critical parts of the complete system (fig. 16) are the resonator (part 15 of fig.16), hot heat exchanger (6 and 7), cold heat exchanger (13 and 12), stack (10) and the speaker (21). All of the above parts have direct impact on the performance of the system. The hot heat exchanger is positioned at the pressure antinode and the velocity antinode is near the closed end. As discussed in the

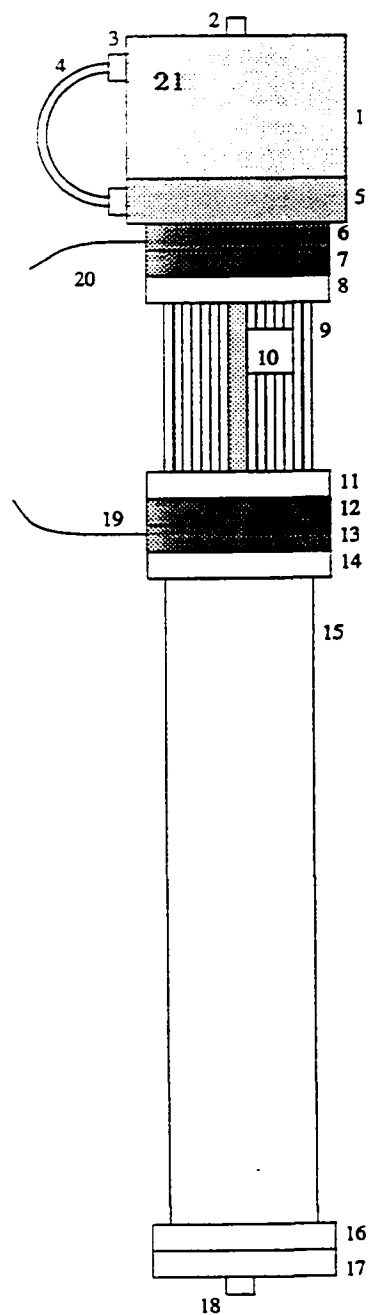


Fig. 16. An overview of the thermoacoustic system used for the experiment with all the major parts numbered (details given in text).

previous chapter, the heat which is absorbed at the cold heat exchanger is given off at the hot heat exchanger. Therefore it is clear that the position of the pressure antinode is critical. Also the thermal contact between the heat exchangers and the heat exchanger sections has to be very good. In fig. 16, part number 1 is the speaker casing, 2 is speaker adaptor, 3 and 4 are the pressure stabilizer connections, 5 is the speaker cover, 6, 7, 12, and 13 are heat exchanger sections, 8, 11, 14 and 16 are the flanges, 9 is stack resonator section, 10 is the stack, 15 is the main resonator, 17 is the end cap, 18 is the end cap connector, 19 and 20 are the thermocouples and 21 is the speaker.

The stack which creates the thermal boundary layer is placed between the two heat exchangers. The gap between the two layers of the stack should be twice the thermal boundary layer thickness. This means that the thermal boundary layer will form on both sides of the stack plate. The position of the pressure antinode and the wavelength are two important criteria for the total length of the system. The length in the present case is  $\lambda/2$  at 500 Hz frequency.

The design of the various complex parts of the apparatus (fig. 16) for the experiment had been made with a view on the flexibility of the workshop at our disposal. There are two sections describing the apparatus, primary and secondary components. Further, the instrumentation required for the measurement of the various parameters will be discussed.

## PRIMARY COMPONENTS

In this section, a detailed discussion of the important parts, which here are called the primary components, will be given. Resonators, heat exchangers and the stack are vital for our experiments as their precision will affect the outcome of the experiments.

The acoustic driver, which is a speaker in our case, is as important as the resonator or other vital parts. Instead of a speaker, a piston/tube arrangement can also be used. The driver apparatus has to be designed to drive a closed, helium-filled vessel at resonance from a point of high impedance, while enabling accurate tuning of the driver frequency over a wide range. The accurate measurements of the driver frequency, power and other variables of this device are critical to the operation of the system. Obviously the diameter of the driver piston (speaker diaphragm) has to fit into the bore of the resonator vessel. Any obstruction to the acoustic wave prior to the heat exchanger and the stack could have a negative effect on the performance of the speaker diaphragm itself. The literature on the description, calculations and design of the acoustic system is extensive. One such literature review which is recommended for the design of an acoustic system applied to thermoacoustic refrigeration is by Hofler (1988).

In the present experiments, the speaker used was a "Realistic 3-inch" midrange tweeter with 30 Watt maximum power output model. The frequency range of the speaker is up to 20,000 Hz, with 8 ohms impedance and 16  $\mu$ F capacitor.

**Resonator**

This is a very vital section in the design of the refrigeration system as in this length of the tube the resonance of the acoustic wave takes place. The resonator vessel (fig.17) is constructed of the acrylic material which has very low thermal conductivity. The low thermal conductivity is desired since a large temperature gradient is expected and the metal tube would conduct most of the heat along the tube material.

Though the leaks were more at joints and seals, other problem with any plastic pressure vessel is its permeability to helium (discussion of helium permeability is given in Appendix C) at room temperature. Due to this the pressure inside the tube will not remain constant and the standing wave condition would be seriously affected over time. This would avoid creation of a heat sink or a heat source (the tube is a large heat sink and heat source). Acrylic material was used for the initial tests as it was very easily available, financially affordable, and was of low thermal conductivity. The internal diameter and the length of this section are 38.1 mm (1.5") and 862.33 mm (33.95") respectively.

**Stack Resonator Section**

A similar discussion as done for the main resonator goes for the stack resonator section (fig. 17). The internal diameter of this section is 38.1 mm (1.5") and its length is 80.01 mm (3.15"). The location of this section along the main resonator can be varied, but fo-

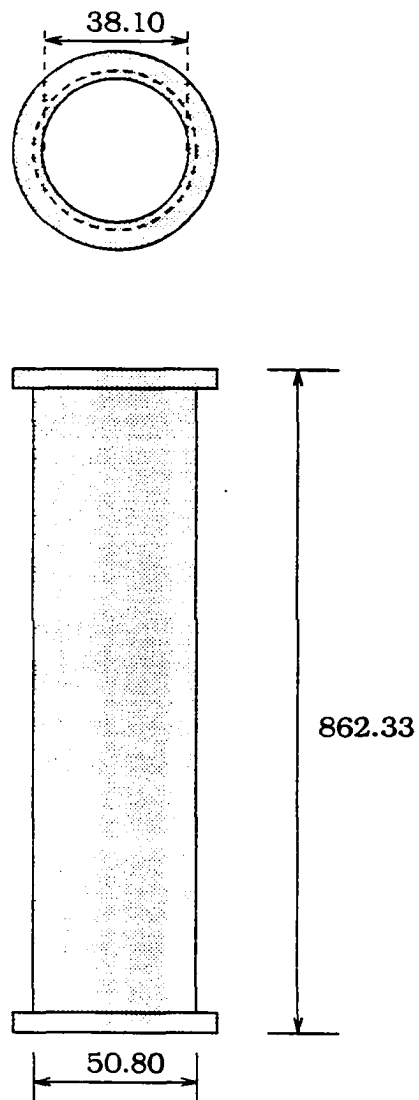


**Fig. 17. The main resonator section made of acrylic tube with dimensions shown in mm.**

r the designed cooling effect it should be placed close to the pressure antinode.

### **Hot and Cold Heat Exchanger Sections**

Each of these sections has two parts made of brass (fig. 18). Each is a ring like section and fits exactly on to the other. A groove is made on each of the sections on the face of the ring closer to the inner surface as shown in fig. 18. This groove when matched with the other groove, creates a gap in which the heat exchanger exactly fits. Care was taken to machine the parts to 0.02 mm (0.001") accuracy. Also the surface has to be perfectly matched with other parts (flanges).

### **Hot and Cold Heat Exchangers**

As the name suggests, the heat exchangers will carry heat from the atmosphere, through the tube, and the heat will be returned to the environment. The heat exchangers play a vital role in the heat transfer, therefore their material, manufacturing technique and shape are very crucial. As discussed in the earlier chapter, heat from one of the heat exchangers is conducted to the gas parcel in the thermal boundary layer of the stack plate. It is then conducted along the length of the stack and conducted back to the other heat exchanger which subsequently conducts back to the atmosphere or the cooling water circulating the heat exchanger. Other design considerations are given in the next chapter where some recommen-

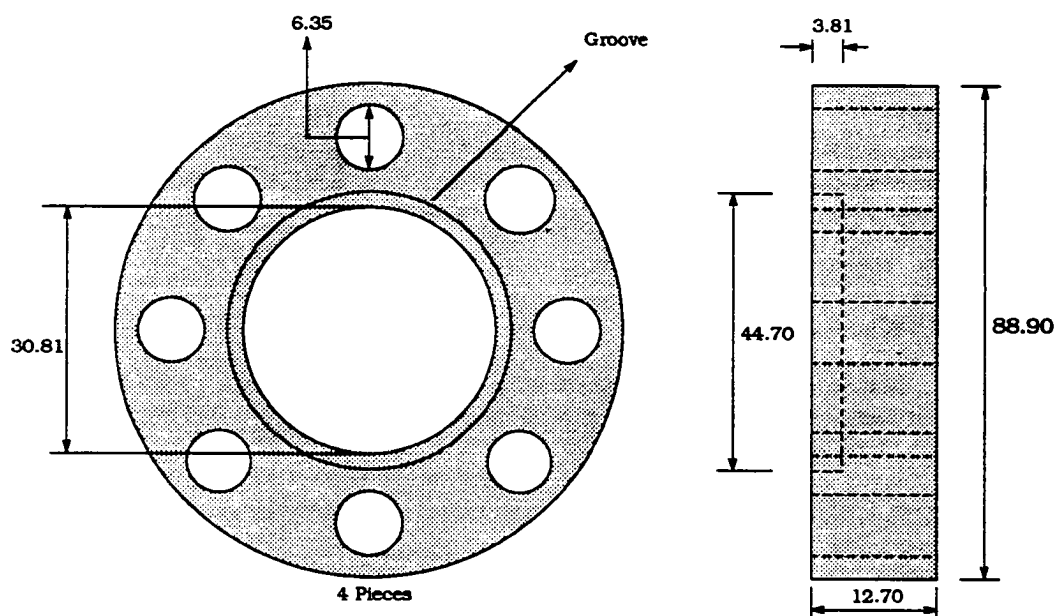


**Fig. 18. Heat exchanger sections made of brass with all details and dimensions (mm) in two different views.**

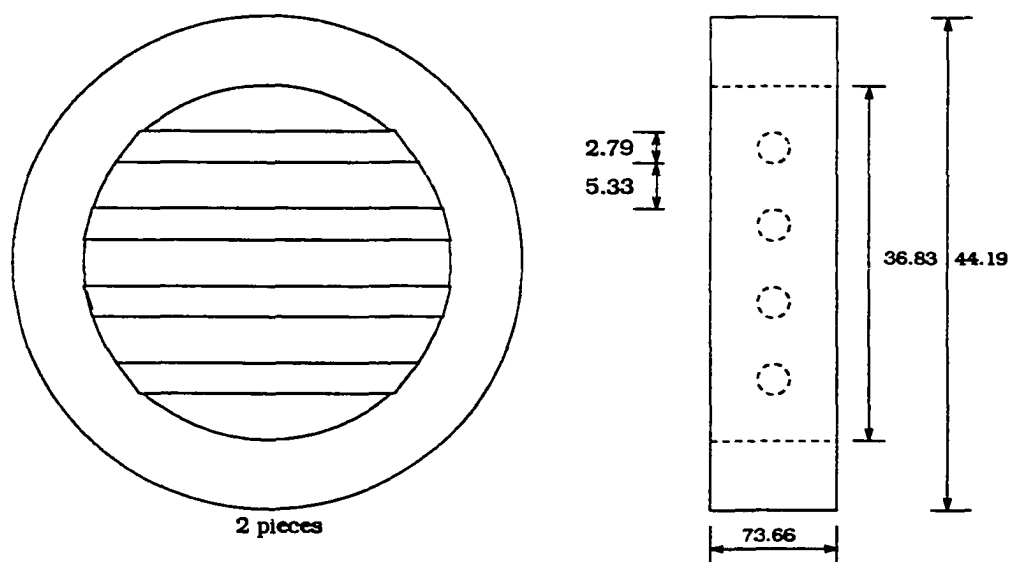


**Fig 19. Heat exchanger made of copper with dimensions (mm) in two different views.**

dations of the design and manufacturing techniques are also discussed.

Making the heat exchangers was very difficult task as it involved very small sizes. The heat exchanger section is a ring-shaped copper piece, which is made from a 32 gauge copper wire (fig. 19). The wire section was converted into a flat rectangular piece and formed into the shape of the ring and the ends were soldered carefully. The internal diameter of the ring is 38.1 mm (1.5") and 4 strips were soldered to the ring. Other dimensions are given in fig. 16.

The circular copper strips were cut and soldered across the diameter of the ring at equal distance as shown in fig. 19. Care was taken to solder the pieces so as to avoid any extra amount of solder on the surfaces of the ring and the strips, which would create turbulence in the fluid.

A very high precision is required to make these parts. One of the high precision methods (Hofler, 1986) to construct the heat exchanger parts is to make a stack of alternating copper and aluminium sheets that are glued together with a thin film of epoxy and electroplated with the height and width of the stack being larger than the bore of the resonator. The stack could then be machined, in a lathe, into a cylindrical volume having a diameter that is the same as the bore of the resonator. The machined outer diameter is then electroplated with copper, thereby joining the edges of all the copper sheets to the plating. The electroplated material is turned down to a specific outer diameter. The face of the cylindrical part is machined until the edges of the copper and aluminium sheets are

exposed, and one or more disk shaped slices are parted off the main part. Finally the aluminium is chemically removed, and the exchanger is ready to be used. Care should be taken to avoid sharp edges which could act as local sites for acoustically stimulated turbulence. A more detailed discussion is given by Hofler (1986).

### **Stack Construction**

The major design considerations for the stack construction are that the spacing between two layers should be at least twice the thermal penetration depth and the width of the stack should be little less ( 0.254 mm or 0.01") than the distance between the two heat exchangers. The material should have low thermal conductivity. A stack of plates (brass sheets of 0.254 mm or 0.01" thick) could be used for comparison of the results with two different thermal conductivities. The plastic sheet should be long enough, so that after it is wound the roll makes a snug fit into the bore of the resonator vessel.

The stack used in our work is a roll consisting of a long strip of spiral wound plastic film (Kapton sheet). This provided the necessary surface area for the thermoacoustic heat transport.

The spiral has many spacers attached on the plastic sheet to maintain a gap between adjacent layers of the spiral. Monofilament fishing line of 0.38 mm (0.014") diameter is used as the spacers. The construction of the stack is very delicate and time consuming as the glue that has to be applied on each fishing line in such a way that the glue does not get thicker than the line itself. Once these spacers are

glued the stack has to be rolled carefully to avoid any contact of the plastic layer with other adjacent layers. The construction of the stack will be explained below.

A spiral roll of the plastic sheet was selected as it is easier to roll around and also it has low thermal conductivity. The sheet is 0.38 mm (0.01496") thick. The plastic sheet was cut from a square piece and care was taken to keep the width of the plastic sheet constant.

Gluing of each spacer (fishing line) is very time consuming if done manually and also not precise. Therefore a jig was used to place the fishing lines parallel to each other and glue them as shown in fig. 20. This jig is a very simple device constructed in the laboratory.

The jig is a flat wooden panel on either side of which an aluminium plate with tooth-like projections was fixed (fig. 20a). Two such plates were fixed on either side of a rectangular wooden panel which is wide enough to allow the film to be laid out along its length.

The plastic film is placed on top of the panel and fixed on either side of its length. The string (fishing line) is fastened to one edge of the jig and then laced back and forth between the teeth of the jig and then fastened at the other end of the jig (fig. 20B). In the region between the two rows of the teeth, the string is precisely aligned parallel to itself.

The jig is a frame that allows access to both sides of the strings. Once the string has been laced properly on top of the plastic film, an adhesive (Polyurethane) is carefully applied on two edges of the string along the length of the film.

A scalpel is then used to cut the strings at the edge of the plastic film. Proper tension in the string is very important. If it is hig-

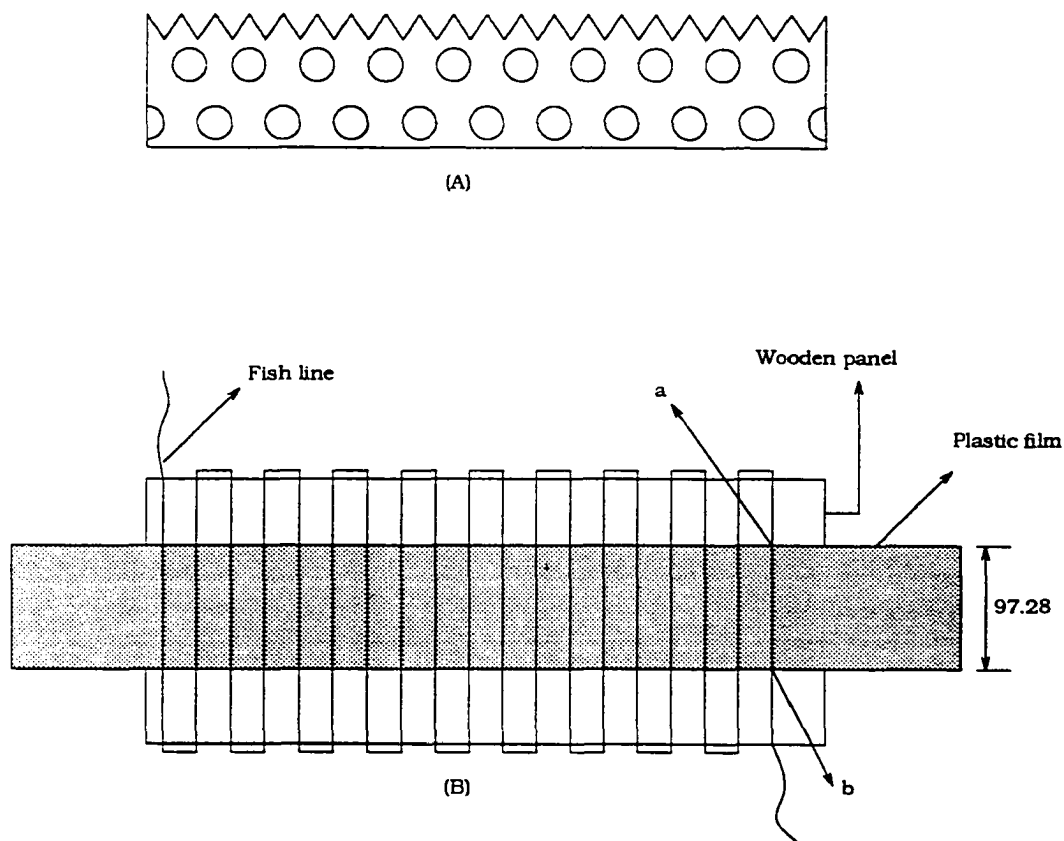


**Fig. 20** The construction of the stack roll. (A) Porous aluminium jig plate with tooth like projections, and (B) spacer strings (monofilament fish line) applied to the structure of the film on the alignment jig. The strings are cut along the length at points 'a' and 'b'.

hly tensed then the string will either get unglued or curl the film and, if very loose, then it will tend to get distorted (the string will not remain parallel to the other neighboring strings).

Each time only a certain length of stack can be prepared since the panel or the jig is not long enough to accommodate the entire length of the stack. Once the glue on certain length is dried, the other length is glued. The time for the glue to dry was about 5-6 hours.

The plastic sheet (film) and the string are then wound around a 6.35 mm (0.25") diameter wooden rod whose length is equal to the width of the film and the distance between the two heat exchangers. Proper care was taken to roll the film. If the roll is wound too tightly, the film will assume a rippled spiral shape rather than a smooth spiral shape, resulting in the inter-layer spacing being too small and non-uniform. The spacing between the strings is 12.7 mm (0.5") and the mean layer spacing is about 0.38 mm (0.01496"). The roll is then pressed carefully between flat surfaces to force the layers to slide with respect to each other until the ends of the roll are straight and square. All this was done very carefully to avoid being pressed more, which would cause the strings to break or become unglued. A total of 5 tries were required to achieve proper dimensions and accuracy. The diameter of the finished roll is adjusted by cutting off the end of the plastic strip until the roll makes a snug fit in the bore of the resonator tube.

## **SECONDARY COMPONENTS**

This section describes the design and construction of the parts which can be called as secondary because they do not directly effect the experiment. However precision construction is important as it will indirectly have an effect on the primary parts.

### **Flanges**

The flanges are made of acrylic sheet of thickness 12.7 mm (0.5"), which was arbitrarily chosen. Each flange is a circular ring whose inner surface makes a snug fit on to the tube's external diameter (50.8 mm, 2") (fig. 21). The outer diameter of the flange is 88.9 mm (3.5"). The ring was fabricated with utmost care as the flange has to fit tight on to the tube, any minute gap left in between the flange and the tube would be a potential leak for the pressurized helium. To make the flange hold tightly to the tube material, an acrylic glue was used, which after applying on to the flange and the tube surface takes about 24 hours to cure. This assembly was tested for its joint strength on the pressing machine. If the dimensions are precise and the glue is evenly spread all along the joint, the assembly would be strong enough to resist about 100 psi pressure.

A flange is attached on either side of the main resonator section and stack resonator sections. Eight bolt holes are drilled along the flange in line with the holes in the heat exchanger sections.

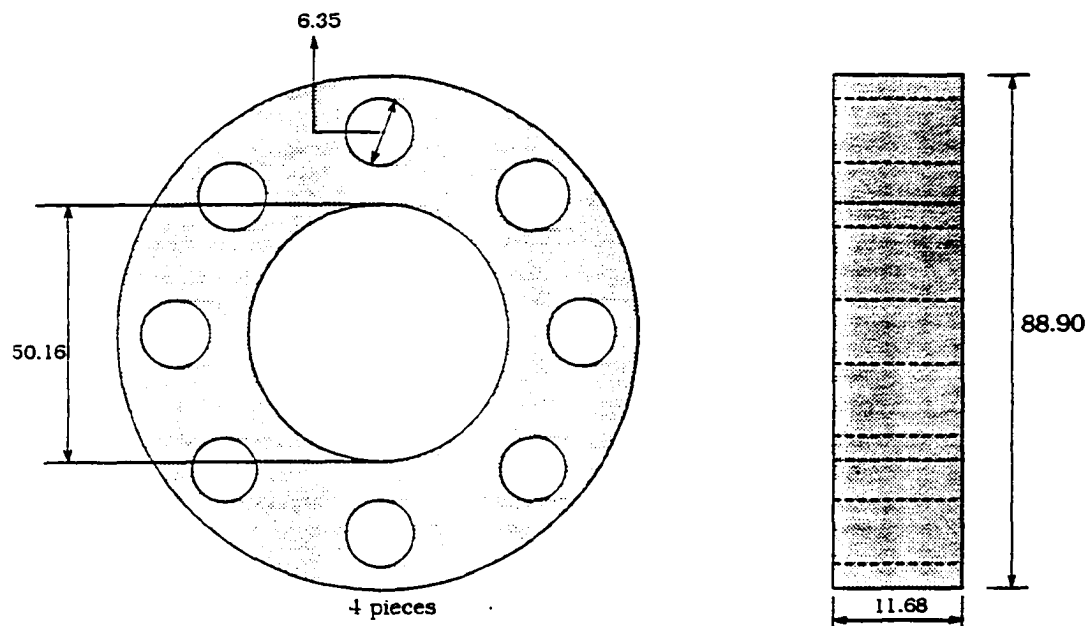


**Fig. 21. Acrylic flanges made of acrylic in two different views with dimensions given in mm.**

### **End Cap**

The end cap is a circular acrylic piece whose outer diameter (88.9 mm, 3.5") is the same as the flanges. The purpose of this is to seal the tube on one end. A solid cylindrical acrylic piece is attached to its center. The diameter of the cylinder (37.592 mm, 1.48") is such that it makes a snug fit into the tube, i.e. the diameter of the cylinder is little less than the internal diameter of the tube (fig. 22).

Threads of 12.7 mm (1/2") diameter are machined through the end cap at its center. These threads pass through the cylinder and the flat piece. The purpose of this bore is to connect the vacuum pump and the helium gas cylinder to the tube.

### **Speaker Casing**

The speaker casing is made of aluminium and designed to cover the speaker (acoustic driver) from all sides in the form of a closed cylinder. The casing has a hole on its back, through which the speaker wiring passes. To make this leak tight, an adaptor is threaded through the hole (fig. 23).

The length (58.92 mm, 2.32") of the casing is slightly longer than the speaker itself. This is done to allow the speaker flange to sit on top of the hollow cylinder walls. 3.17501 mm (1/8") taper screw threads are drilled in the cylinder walls in line with the holes of the speaker flange.

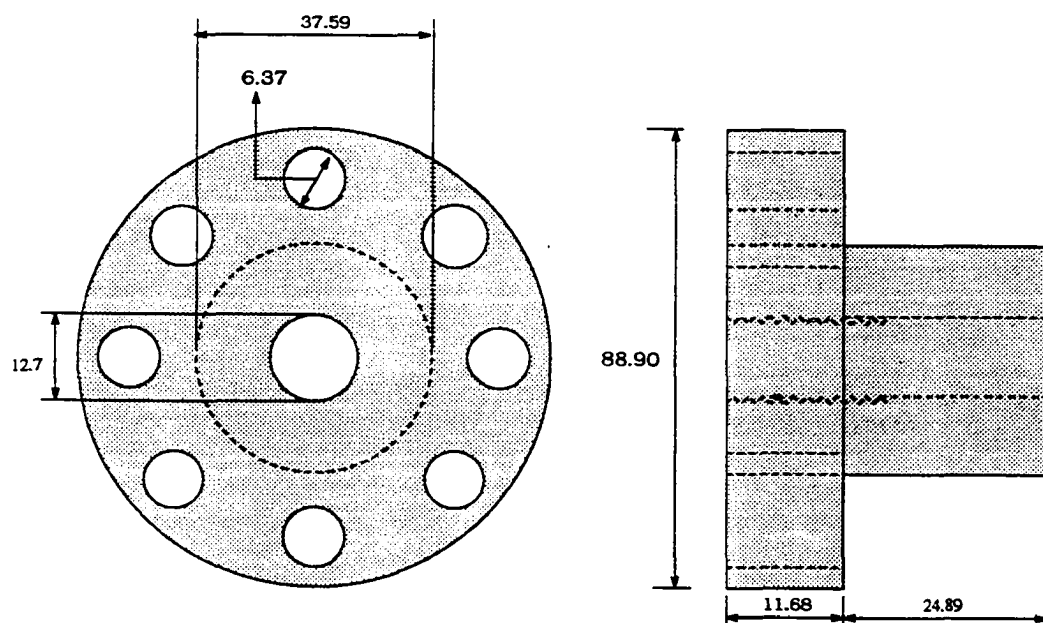


**Fig. 22.** End cap made of acrylic with thread connection for the vacuum pump and helium with dimensions in mm.

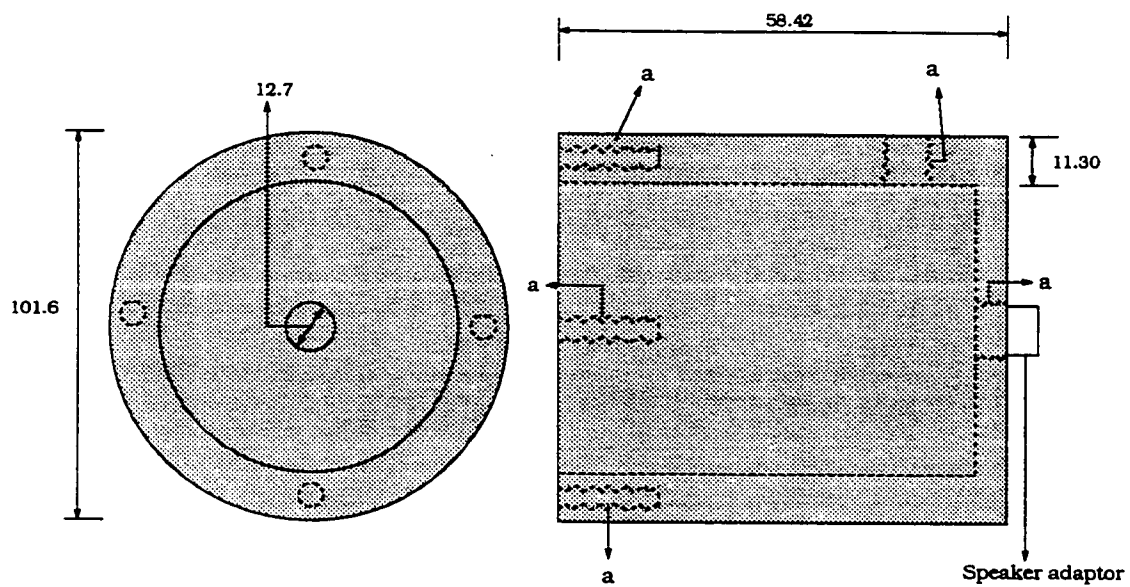


Fig. 23. Speaker casing made of aluminium shown in two different views with the threads drilled at positions shown by 'a' with dimensions in mm.

### **Speaker Casing Cover**

The cover is also made of aluminium in the shape of a ring with internal diameter the same as that of the tube and the external diameter matching the casing. The speaker casing has a thickness of 23.31 mm (0.918") (fig. 24). Four holes are drilled in line with the speaker casing and the speaker itself. When all of this parts, i.e., the speaker casing, the speaker and the speaker casing cover, are in line, they can be held together by 3.17501 mm (1/8") screws.

The wavelength of the acoustic wave is measured from the attachment point of the speaker casing and the cover to the end of the tube (end cap).

A problem with the above geometry is that when all the parts of the tube are assembled, the helium pressures on the back of the speaker and in the front are different. This is due to the pressure differential created by the increased pressure applied by the helium in the front of the speaker and the atmospheric pressure unchanged on the back of the speaker. Due to this pressure differential the speaker diaphragm may break. The above problem may conveniently be avoided by equalizing the pressure on both sides. In our case this problem is overcome by attaching a tube, external to the assembly. Two holes, one is drilled across the speaker casing cover material and the other is drilled on the speaker casing at its back portion as shown in fig. 24.

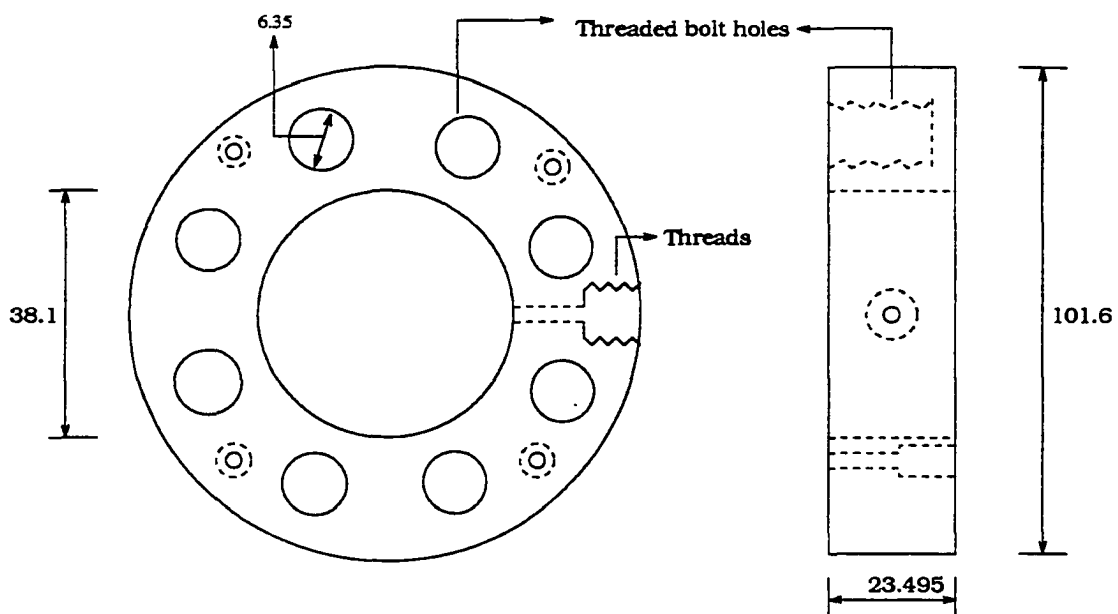


Fig. 24. Speaker cover was made of aluminium and had the connection shown for the pressure equalizer. Dimensions are in mm.

## **INSTRUMENTATION**

In this section, we will discuss about the various electronics, pressure regulators and the acoustic equipment used for the experiments. Each of these parts are vital to our experiments as their precision would determine the accuracy of the results.

The pressure regulator used was a two dial regulator. Dial A reads the pressure inside the helium cylinder and the dial B reads the outlet pressure. As shown in fig. 25 the connection from the tube end (end cap) is a 'T' connection. One leg of the 'T' is connected to the helium cylinder through the regulator and the other leg is connected to the vacuum pump through a valve. When this valve is open, the tube can be vacuumed; when the valve is closed, with the regulator in the open position, the tube can be pressurized with helium.

A vacuum pump (GE 1/3 HP, centrifugal, V115 type) was used to evacuate the chamber prior to the admission of He.

On the back side of the tube (speaker end), the speaker adaptor is connected to an amplifier (Realistic, MPA-95, 100 watt, P.A.).

The amplifier is connected to a frequency generator (BK Precision Dynascan Corporation 3010 Function generator). The range of frequency it can generate is from 0.001 - 1000 KHz.

To accurately read the frequency, the generator is connected to a frequency counter (B K precision Dynascan Corporation 1805 80 MHz type) which digitally displays the frequency generated. The accuracy of the counter is 0.01 Hz. The frequency range which can be

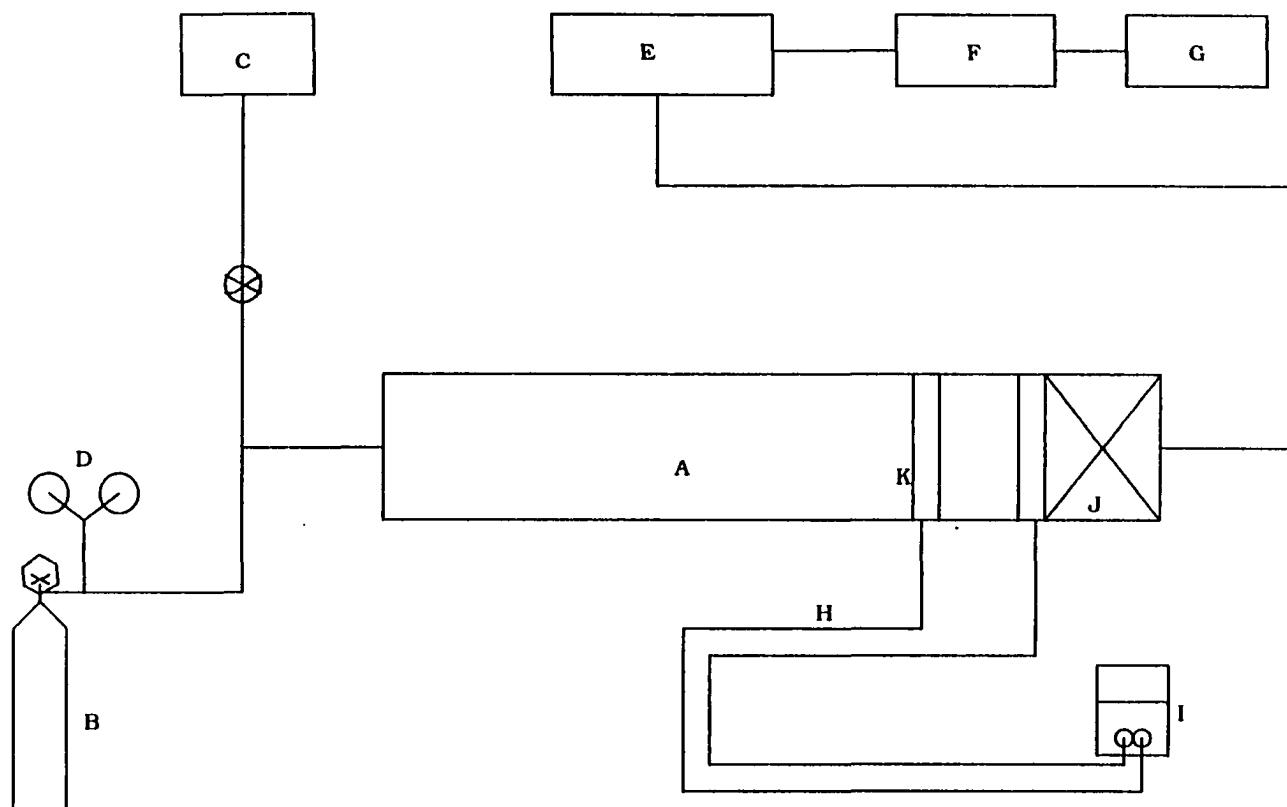


Fig. 25. Block diagram showing various components in the thermoacoustic refrigeration system used in this work. A. tube, B. helium cylinder, C. vacuum pump, D. pressure regulator, E. amplifier, F. frequency generator, G. frequency counter, H. thermocouple leads, I. digital thermometer, J. speaker, K. heat exchanger sections.

measured is 0.01 Hz - 80 MHz.

When the frequency is fixed by the generator, the signal goes to the amplifier, where the signal is amplified to the required level and then sent to the speaker. The frequency generator can be adjusted to give a sinusoidal wave or a square wave form. It has a wheel-like knob through which the required frequency can be adjusted with the help of the counter, which would display the frequency fixed. The amplitude can also be adjusted through the frequency generator.

The temperatures of each heat exchanger are monitored with two type-K thermocouples. One junction is inserted into the heat exchanger section from outside by drilling a hole about half an inch inside the section. The leads from the thermocouples were plugged into a digital temperature indicator (Keithley 870 Digital Thermometer), which reads the temperatures from K-type thermocouples up to 2000 °F (1370 °C). The accuracy of this thermometer was adjusted by comparing the atmospheric temperature read by an ordinary mercury thermometer and "Omega type-T temperature indicator" (stand alone thermocouple indicator).

## **CHAPTER 5**

# **EXPERIMENT AND RECOMMENDATIONS**

### **INTRODUCTION**

In this chapter, the assembly of the apparatus described in the previous chapter and the test run of the thermoacoustic refrigerator will be discussed. Further, recommendations to rectify some of the problems associated with the present design will be made.

### **ASSEMBLY**

The assembly of the apparatus was done very carefully so as to avoid any damage to the various parts, specially the speaker and the speaker casing. The flanges are mounted on the tube and fixed with acrylic glue (Weld On, Acrylic Sealant, IPS Corp.). The sealant was applied on both mating surfaces with the help of an injector. Since the glue evaporates very fast, the flange and the tube were mounted immediately. After clamping the joint, it was left to dry for 24 hours till the joint is held rigidly. Similarly all the flanges were mounted and fixed to the tube.

The gaskets used for leak proof seal were cut from a square 0.0625" thick neoprene sheet. Each of the gasket was cut into a circular piece and the holes for the bolts to pass were drilled. During the assembly an appropriate quantity of "high temperature, red silicone sealant" was applied on both faces of the gasket to seal all the crevices left over by the gasket. The silicone sealant after being left to dry for 24 hours seals into a thin rubber like sheet. Special care was taken to avoid the spill of the sealant on to the speaker parts during the assembly of the speaker parts. The gap between the heat exchanger and the heat exchanger sections was filled with heat sink material (Silicone heat sink compound), to avoid any air gap that would adversely effect the heat transfer from the heat exchanger to the surface of the resonator.

## **TEST RUN**

The above experimental setup was designed to operate at 10 bar helium pressure and 500 Hz frequency. But the test experiment ran into several problems even at the lower pressures. One of the major difficulties was to make the apparatus leak proof for pressurized helium gas. Since the gas is highly diffusive, it was leaking out from the joints between flanges and the tube, flanges and the neighboring heat exchanger sections and holes drilled for the bolts. Even after several test trials the maximum pressure that could be reached without any leaks was 2 bar. The results at such a low pressure were very inconsistent and showed no signs of refrigeration. Each of the trials involved de-assembly of the complete setup.

preparation of new gaskets, applying the heat sink compound, the acrylic glue and the red silicone sealant, and re-assembly of the apparatus parts. At every occasion, care was taken to seal all the potential leak areas by applying appropriate amount of red sealant. At one such trial, higher helium pressure (3 bar) was reached, which is still less than the designed 10 bar. The results were still very inconsistent. During each trial run, the experiment was left in running position till the temperature rise due to the heat generated by the driver reached steady state. It normally takes 10 to 12 hours to stabilize. The readings were recorded every half hour.

Here detailed recommendations will be made for any future design and testing.

## **RECOMMENDATIONS**

As discussed earlier the design of a thermoacoustic refrigerator involves design and fabrication of very small components and their dimensions are very critical to the performance of the refrigerator. Every component has to be designed in accordance with their importance in the outcome of the results. This means that the components which directly affect the heat transfer and also the resonance have to be very precise. The material of these components is also vital and their manufacturing technique would effect the outcome. The finish of the parts is particularly important as any roughness or burrs would effect the fluid mechanics of the acoustic flow.

In this section, each of the component dimensions, their finish, manufacturing technique and other design aspects will be dealt with in detail. Most of these aspects were understood only after going through the design and conducting experiments with the available workshop and lab flexibility.

### **Primary Components**

In this section the recommendations for the important parts like resonators, heat exchangers and the stack will be discussed.

#### **Resonator**

The shape and the material of this section have a direct bearing on the results. There are several shapes that can be used in a refrigerator. One such shape where the desired resonance and better heat transfer can be achieved is by placing a spherical volume at  $\lambda/4$  point in a  $\lambda/2$  resonator. Due to the acoustic streaming, there could be a substantial heat load on the cold heat exchanger which could be reduced by the spherical volume. Several such geometries and their design considerations are discussed in detail by Hofler (1986), where he also discusses the dimensions of the above spherical geometry. Such a spherical shape was not considered here due to the manufacturing and fabrication difficulties. The fabrication of various joints includes the soldering of the spherical section to the tube section.

The material of the resonator is very important as it will affect the heat transfer and change the quantity of heat load on the cold heat exchanger. The section of the resonator which contains the stack is subjected to a large temperature gradient during the operation and therefore should have low thermal conductance. The lowest conductance can be found with plastic material, therefore fiberglass material could be used. Elsewhere the vessel could be made of heavy gauge copper or stainless steel.

A method to reduce the helium diffusion through the fiberglass is to have a metal film sandwiched between two layers of fiberglass. This has been found to reduce the leak by a factor of 10. The details of how this can be done is given by Hofler (1986).

The more the number of joints, the higher the potential of leaks, as the joints provide a high potential for the helium to diffuse. Therefore it is suggested that the number of joints should be reduced to a minimum.

Another important factor to be considered during the design of a resonator is to see that the inner surface is as smooth as possible, since any rough or uneven surface would substantially change the acoustic and fluid flow. The uneven projections would be a potential local turbulent point which is highly undesirable.

### **Heat Exchangers**

These sections are very important as the heat transfer with the atmosphere takes place at these points. The material of these sections should have a very high thermal conductance. Therefore

brass was used. The strips are made of copper; their size and shape will be discussed in this section. Overall the design objective is to maximize heat transfer without disturbing the flow greatly.

The number of strips in a heat exchanger will have direct impact on the acoustic flow. If the numbers of strips are large, the acoustic flow will be obstructed; if they are less, the heat transfer will be affected, as these strips carry the heat from the stack to the atmosphere. The diameter of the strips may vary but care must be taken to optimize them so that more strips may be fit in the diameter. Very thin strips may have a deleterious effect on the heat transfer. Finally the edges of the strips should be rounded off, as any square edge may create local turbulence in the flow.

It is critical to have good thermal contact between the heat exchanger and the heat exchanger section. All gaps should be filled with suitable heat sink compound.

### **Stack**

The length of the stack has to be less than the distance between the heat exchangers by approximately 0.1-0.2 mm on each side of the stack. The gap between two layers of the stack has to be constant without too many distortions. Finally, the stack should make a snug fit into the bore of the resonator.

### **Other Considerations**

The major problem with the present design was its leakage of Helium. This can be corrected in several ways, one of which is to replace the neoprene gaskets with O-rings. The O-rings have been proven to seal the joints up to several 100 psi. These O-rings have to be grooved below the bolt holes so that the helium does not leak through the bolt holes. Another potential point of leak is the joints between flanges and the tube. If the joints are plastic welded, these leaks can be reduced considerably. Also if gaskets have to be used, they should be sufficiently thick, so as to withstand high pressure applied by the bolts, without getting torn.

The end cap in the present design has a hole drilled for vacuuming and pressurizing the tube. This hole may pose an uneven surface and would seriously affect the acoustic waves and their resonance inside the tube. This problem could be tackled by placing this connection at the back of the speaker in the speaker casing. To avoid any contamination of the helium gas with air molecules the evacuation and pressurizing should be repeated several times before the system is brought up to the desired pressure. The rate of pressurizing and de-pressurizing must be low to avoid any damage to the speaker diaphragm and the stack.

To absorb the heat transferred from the cold heat exchanger and the heat generated by the acoustic driver, cooling pipes should be provided. The cooling pipes may be soldered on top of the hot heat exchanger, which will transfer the heat from the heat exchanger to the atmosphere by circulating water at atmospheric temperature.

If microphones are provided at different positions in the resonator, the pressure amplitude can be measured experimentally. Also two more thermocouples should be attached in the center of each of the heat exchangers. These thermocouples will help measure the temperature at the center. The typical temperature difference between the center of the heat exchanger and the wall is 2 °C.

## **CONCLUSION**

The application of acoustic waves in a closed and controlled environment can lead to cooling and heating effects. When a standing wave is imposed in a tube, with the help of resonance, the heat can be transported from one point to another. Such an acoustic system has only one moving part, i.e. speaker diaphragm, which makes it easy to operate and maintain. Though acoustic waves generally produce minute temperature changes, these changes can be exaggerated considerably with the help of stack plates (spirally wound plastic stack layers). The stack layers create thermal boundary layers adjacent to their surfaces. The overall cycle undergoes two constant temperature and two isobaric processes (constant pressure).

A numerical simulation indicated that for constant thermophysical properties and a given radius of the tube, maximum energy flux is achieved only at one particular frequency and it is proportional to the square of the radius. The acoustic pressure also has affect on the results. The energy flux increases with pressure, but the acoustic work required also increases. The coefficient of performance increases only up to a certain pressure and than

stabilizes. Helium is used as the working fluid due to its high conductivity, low viscosity, low Prandtl number, high thermal expansion coefficient and availability.

To verify the above theory, an experiment was modelled, designed and fabricated in the lab. The experiment ran into several problems with the leakage of the seals and joints. Even after several attempts the problem of leaks could not be fixed. With better seals and fewer joints, it is possible to make the system work, but it could not be done here due to time and other constraints. Therefore some detailed recommendations are made for any future undertaking of the project. They are,

1. The number of joints should be reduced to the minimum.
2. The joints must be strong, plastic welded if possible.
3. Using gaskets with sealant material may not work, a possible alternative is to use O-rings.
4. The construction of the resonator, stack and heat exchangers has to be precise in the dimensions and material, eg. the gap between the layers of the stack has to be precise.
5. Care should be taken while pressurizing the tube, it may damage the speaker diaphragm. Locate the helium entry hole at the back of the speaker casing if possible.

As seen from the analysis, it can be concluded that this new technology of thermoacoustic refrigeration can be an efficient method like other refrigeration systems, eg., vapor compression systems. An advantage of the acoustic system is that it does not cause any damage to the atmospheric ozone, like the present CFC systems.

It is quite possible that with further research the acoustic refrigeration system could conceivably replace current vapor compression systems.

## NOMENCLATURE

$A$	= Amplitude
$a$	= Sound speed
$cop$	= Coefficient of performance
$C_p$	= Isobaric heat capacity per unit mass
$C_v$	= Constant volume heat capacity
$d$	= Tube diameter
$f$	= Frequency
$H$	= Entahlpny
$h$	= Half plate spacing
$K$	= Thermal conductivity
$l$	= Half plate thickness
$L$	= Tube length
$Pr$	= Prandtl number
$P$	= Pressure
$Q$	= Heat flux
$q$	= Heat flux per unit area
$R$	= Tube radius or Gas constant
$s$	= Entropy
$T$	= Temperature
$u$	= x component of velocity
$v$	= y component of velocity
$W$	= Work or acoustic power
$x$	= Axial direction along the tube
$y$	= Perpendicular direction to the axis of the tube
$\beta$	= Thermal expansion coefficient
$\gamma$	= Specific heat ratio
$\Delta x$	= length of the plate
$\delta$	= Penetration depth

$\varepsilon_s$	= Plate heat capacity ratio (ratio of heat capacity of fluid to the plate. $(\rho_m C_p \delta_k / \rho_f C_f \delta_f)$ )
$\kappa$	= Thermal diffusivity
$\lambda$	= Wavelength
$\lambda$	= Radian wavelength
$\mu$	= Dynamic viscosity
$\nu$	= Kinematic viscosity
$\psi$	= Normalized temperature gradient
$\Pi$	= Perimeter
$\rho$	= Density
$\omega$	= Angular frequency
$\nabla$	= Gradient

### Subscripts and Superscripts

A, a	= Amplitude
C	= Carnot or cold
cr	= Critical
H	= Hot
f	= Plate or film
m	= Mean
o	= First order
s	= Standing wave conditions
$\kappa$	= Thermal
$\nu$	= Viscous
1	= First order
2	= Second order

## BIBLIOGRAPHY

- Beranek, L.L., 1971, *Noise and Vibration Control*, McGraw Hill, New York.
- Galiullin, G. and Khalimov, G.G., 1985, "Experimental study of heat transfer in a tube with large amplitude resonance oscillations," *Invertiya VUZ. Aviatrsionnaya Tekhnika*, v. 28 (2), pp. 15 - 18.
- Garrett, S.L. and Hofler, T.J., 1991, "Thermoacoustic refrigeration," Preprint from Technology 2001: The Second National Technology Transfer Conference and Exposition, San Jose, CA.
- Garrett, S.L. and Hofler, T.J., 1992, December, "Thermoacoustic refrigeration," *ASHRAE Journal*, pp. 28 - 36.
- Grassman, P.P. and Tuma, M., 1979, "Applications of the electrolytic method-II, mass transfer within a tube for steady, oscillating and pulsating flows," *Int. J. Heat Mass Transfer*, v. 22, pp. 799 - 804.
- Ha, M.Y. and Yavuzakurt, S., 1993, "A theoretical investigation of acoustic enhancement of heat and mass transfer-I, Pure oscillating flow," *Int. J. Heat Mass Transfer*, v. 36 (8), p. 2183 - 2192.
- Ha, M.Y. and Yavuzakurt, S., 1993, "A theoretical investigation of acoustic enhancement of heat and mass transfer-II, Oscillating flow with a steady velocity component," *Int. J. Heat Mass Transfer*, v. 36 (8), pp. 2193 - 2202.
- Handbook of Chemistry and Physics*, 1973, 55th edition, CRC press, Ohio.
- Hofler, T.J., 1986, "Thermoacoustic refrigerator design and performance," Ph.D. thesis, University of California, San Diego.
- Hofler, T.J., 1988, "Accurate acoustic power measurements with a high intensity driver," *J. Acoust. Soc. Am.*, v. 83 (2), pp. 777 - 786.
- Joshi, C.H., Kamm, R.D., Drazen, J.M. and Slutsky, A.S., 1983, "An experimental study of gas exchange in laminar oscillatory flow," *J. Fluid Mech.*, v. 133, pp. 245 - 254.

- Kinsler, L.E., Austin, R.F., Coppens, A.B. and Sanders, J.V., 1982, *Fundamentals of Acoustics*, 3rd edition, John Wiley and Sons, New York.
- Kurzweg, U.H. and Zhao, L.D., 1984, "Heat transfer by high frequency oscillations: A new hydrodynamic technique for achieving large effective thermal conductivities," *Phys. Fluids*, v. 27 (11), pp. 2624 - 2627.
- Kurzweg, U.H. and Chen, J., 1988, "Heat transport along an oscillating flat plate," *J. Heat Transfer*, v. 110, pp. 789 - 790.
- Kurzweg, U.H., 1985, "Enhanced heat conduction in fluids subjected to sinusoidal oscillations," *J. Heat Transfer*, v. 107, pp. 459 - 462.
- Kurzweg, U.H., 1986, "Temporal and spatial distribution of heat flux in oscillating flow subjected to an axial temperature gradient," *Int. J. Heat Mass Transfer*, v. 29(12), pp. 1969 - 1977.
- Kurzweg, U.H., 1985, "Enhanced heat conduction in oscillating viscous flows within parallel plate channels," *J. Fluid Mech.*, v. 156, pp. 291 - 299.
- Landau and Lifshitz, 1987, *Fluid Mechanics*, 2nd edition, Pergamon press, Oxford, v. 6.
- London, F., 1954, *Superfluids*, Dover Publications, New York, v. II.
- Merkli, P. and Thomann, H., 1975, "Thermoacoustic effects in a resonance tube," *J. Fluid Mech.*, v. 70, pp. 161 - 179.
- Merkli, P and Thomann, H., 1975b, "Transition to turbulence in oscillating pipe flow," *J. Fluid Mech.*, v. 68, pp. 567.
- Ozawa M. and Kawamoto, A., 1991, "Lumped parameter modeling of heat transfer enhanced by sinusoidal motion of fluid," *Int. J. Heat Mass Transfer*, v. 34(12), pp. 3083 - 3095.
- Pauly S., 1989, *Polymer Handbook*, 3rd edition, Bandrup J. and Immergut E.H., Wiley-Interscience, New York, Sec. VI, pp. 435-438.
- Repin, V.B., 1985, "Heat transfer associated with viscous two dimensional channel flow in a transverse acoustic field," *Izv. Akad. Nauk SSSR, Mekh. Zhidk. Gaza*, v. 20, pp. 369 - 377.
- Rott, N., 1969, "Damped and thermally driven acoustic oscillations in wide and narrow tubes," *Z. Angew. Math. Phys*, v. 20, pp. 230 - 242.

Rott, N., 1973, "Thermally driven acoustic oscillations. part II: Stability limit for helium," Z. Angew. Math, Phys, v. 24, pp. 54 - 71.

Rott, N., 1975, "Thermally driven acoustic oscillations, part III: Second order heat flux," Z. Angew Math. Phys., v. 26, pp. 43 - 48.

Rott, N., 1984, "Thermoacoustic heating at the closed end of an oscillating gas column," J. Fluid Mech., v. 145, pp. 1 - 9.

Sigel, R., 1987, "Influence of oscillation induced diffusion on heat transfer in a uniformly heated channel," Trans. ASME., v. 109, pp. 244 - 247.

Swift, G.W., 1988, "Thermoacoustic engines," J. Acoust. Soc. Am., v. 84 (4), pp. 1145 - 1180.

Wheatley, J., Hofler, T.J., Swift, G.W. and Miglori, A., 1983, "An intrinsically irreversible thermoacoustic heat engine," J. Acoust. Soc. Am., v. 74 (1), pp. 153 - 170.

Wheatley, J., Hofler, T.J., Swift, G.W. and Miglori, A., 1986, Fall, "Natural heat engines," Los Alamos Science, No. 14, pp. 1 - 33.

White, F.M., 1986, *Fluid Mechanics*, 2nd edition, McGraw Hill, New York.

Yagaya, S. and Smith, J.L., Jr., 1991, "A study of gas spring heat transfer for non-sinusoidal piston motion," ASME Winter Annual Meeting, Atlanta, GA.

Yazaki, T., Sugiooka, S., Mizutani, F. and Mamada, H., 1990, "Nonlinear dynamics of a forced thermoacoustic oscillation," The American Physical Society, v. 64, pp. 2515 - 2518.

## **APPENDIX A**

### **FORTRAN PROGRAM**

C THIS IS A FORTRAN PROGRAM TO COMPUTE ENERGY FLUX AND  
C ACOUSTIC WORK AT DIFFERENT FREQUENCIES AND THIS  
C PARTICULAR PROGRAM WITH LITTLE VARIATION WOULD GIVE  
C THE ENERGY FLUX AND ACOUSTIC WORK FOR VARIABLE  
C PRESSURE.

```
REAL L1,KS2,K2,LA(1000),LB(1000),COP(1000)
DIMENSIONF(1000),W(1000),PS1(1000),US1(1000),
DIMENSION DK(1000),DV(1000), DS(1000), DTC(1000)
DIMENSION WO(1000),H(1000),ES(1000),TT(1000),
DIMENSION X1(1000,100)
OPEN (10, FILE = 'RESULTS', STATUS = 'NEW')
```

C MEAN TEMPERATURE TM (°K), MEAN PRESSURE PM (bar)

TM = 255

PM = 10

C TMB IS THE PRODUCT OF MEAN TEMPERATURE AND THERMAL  
C EXPANSION COEFFICIENT.

TMB = 1

C G IS SPECIFIC HEAT RATIO CP/CV

$$G = 1.67$$

$$CP = 5200$$

C RHO IS THE PRANDTL NUMBER FOR HELIUM.

$$RHO = 0.68$$

C RM IS DENSITY OF GAS

$$RM = 1.9$$

C K IS THERMAL CONDUCTIVITY OF GAS

$$K2 = 0.13$$

C KS IS THERMAL CONDUCTIVITY OF PLATE (STACK) MATERIAL.

$$KS2 = 0.16$$

C RS IS DENSITY OF PLATE MATERIAL

$$RS = 1400$$

C CS IS SPECIFIC HEAT OF PLATE

$$CS = 1100$$

C PA IS PRESSURE AMPLITUDE

$$PA = 30000$$

C DT IS CHOSEN TEMPERATURE DIFFERENTIAL ACROSS THE  
C PLATE

$$DT = 90$$

C YO IS HALF PLATE SPACING

$$YO = 0.00019$$

C L IS HALF PLATE THICKNESS

$$L1 = 0.00004$$

C DX IS PLATE LENGTH

$$DX = 0.08$$

C R IS TUBE DIAMETER

$$R = .019$$

C A IS THE SPEED OF SOUND IN THE GAS

$$A = 940$$

C DTM IS DIFFERENCE OF TM AND DT

$$DTM = 165$$

C CALCULATION OF CONSTANT PI ( $\pi$ )

$$pi = 4 * ATAN(1.0)$$

C ITERATION FOR FREQUENCIES FROM 470 TO 600.

$$DO 100 I = 470, 600, 10$$

$$F(I) = I$$

C ANGULAR FREQUENCY

$$W(I) = 2 * PI * F(I)$$

C WAVE LENGTH

$$LA(I) = A / F(I)$$

C RADIAN WAVE LENGTH

$$LB(I) = LA(I) / (2 * PI)$$

C ITERATION FOR THE POSITION OF THE STACK

$$H1 = 0.0$$

$$WO1 = 0.0$$

$$DO 110 J = 1, 79$$

$$X1(I, J) = 0.01 * J * PI * LB(I)$$

C CALCULATION OF FIRST ORDER PRESSURE AMPLITUDE AND

C VELOCITY AMPLITUDE OF THE STANDING WAVE

$$PS1(I) = PA * SIN(X1(I, J) / LB(I))$$

$$US1(I) = (1 + L1 / YO) * (PA / (RM * A)) * COS(X1(I, J) / LB(I))$$

C CRITICAL TEMPERATURE GRADIENT FROM REF.(SWIFT,1988)

$$DTC(I) = (TMB * W(I) * PS1(I)) / (RM * CP * US1(I))$$

C TEMPERATURE RATIO OF DT AND DTC

$$TT(I) = DT/(DX*DTC(I))$$

C THERMAL PENETRATION DEPTH

$$DK(I) = (SQRT(K1/(PI*F(I)*RM1*CP)))$$

C VISCOUS PENETRATION DEPTH

$$DV(I) = DK(I)*SQRT(RHO)$$

C PLATE THERMAL PENETRATION DEPTH

$$DS(I) = (SQRT(KS1/(PI*F(I)*RS*CS)))$$

C PLATE HEAT CAPACITY RATIO

$$ES(I) = (RM1*CP*DK(I))/(RS*CS*DS(I))$$

C PERIMETER ON WHICH HEAT TRANSFER IS ACTIVE

$$PP = (PI*R**2)/(YO+L1)$$

C ENERGY FLUX

$$\begin{aligned} H(I) = & -((PP*DK(I)*TMB*PS1(I)*US1(I))/(4*(1+ES(I))*(1+RHO) \\ + & *(1-DV(I)/YO+DV(I)**2/(2*YO**2))))*((TT(I)*(1+SQRT(RHO) \\ + & +RHO+RHO*ES(I))/(1+SQRT(RHO))-(1+SQRT(RHO)-DV(I)/YO) \\ + & )-PP*(YO*K2+L1*KS2)*(DTM/X1(I,J)) \end{aligned}$$

C ACOUSTIC WORK

$$\begin{aligned} WO(I) = & ((PP*DK(I)*DX*(G-1)*W(I)*PS1(I)**2)/(4*RM*A**2*( \\ + & (1+ES(I))))*((TT(I)/((1+SQRT(RHO))*(1-DV(I)/YO+DV(I)**2/ \\ + & (2*YO**2))))-1)-(PP*DV(I)*DX*W(I)*RM*US1(I)**2)/(4*(1- \\ + & DV(I)/YO+DV(I)**2/(2*YO**2))) \\ WO(I) = & -WO(I) \end{aligned}$$

IF (H1.LT.H(I).AND.WO1.LT.WO(I)) THEN

```
H1=H(I)
WO1=WO(I)
ELSE
GO TO 110
ENDIF
110  CONTINUE
C COEFFICIENT OF PERFORMANCE RATIO, COP/COP(CARNOT)
      COP(I) = H1/WO1

100      CONTINUE

      DO 150 I = 470, 600,10
      WRITE(10,20)  I, H1, WO1, COP(I)
20      FORMAT(5F6.3)
150      CONTINUE
      STOP
      END
```

## APPENDIX B

The solution of the equation to calculate the velocity field in the acoustic wave is illustrated here. As equation (13) is non-homogeneous, the solution is obtained by applying the separation of variables technique.

The governing equation is,

$$i\omega\rho_m u_1 = -\frac{\partial P_1}{\partial x} + \mu \frac{\partial^2 u_1}{\partial y^2}$$

This equation can be rewritten as,

$$\frac{\partial^2 u_1}{\partial y^2} - \frac{i\omega\rho_m}{\mu} u_1 = -\frac{1}{\mu} \frac{\partial P_1}{\partial x} \quad (1)$$

With boundary conditions,

$$u_1(h) = u_1(-h) = 0 \quad (2)$$

After separation of variables, we will have,

$$u_1 = A_1 e^{y\sqrt{i\omega\rho_m/\mu}} + A_2 e^{-y\sqrt{i\omega\rho_m/\mu}} - \frac{1}{i\omega\rho_m} \frac{dP_1}{dx} \quad (3)$$

where  $A_1$  and  $A_2$  are constants. Applying the boundary conditions the above equation becomes,

$$u_1 = A_1 e^{y\sqrt{i\omega\rho_m/\mu}} + A_2 e^{-y\sqrt{i\omega\rho_m/\mu}} - \frac{1}{i\omega\rho_m} \frac{dP_1}{dx} = 0 \quad (4)$$

and

$$u_1 = A_1 e^{-y\sqrt{i\omega\rho_m/\mu}} + A_2 e^{y\sqrt{i\omega\rho_m/\mu}} - \frac{1}{i\omega\rho_m} \frac{dP_1}{dx} = 0 \quad (5)$$

Solving the above two equations, we get the values for the constants,

$$A_1 = \frac{1}{i\omega\rho_m} \frac{dP_1}{dx} \frac{(1 - e^{-2h\sqrt{i\omega\rho_m/\mu}})}{e^{-2h\sqrt{i\omega\rho_m/\mu}}(1 - e^{-4h\sqrt{i\omega\rho_m/\mu}})} \quad (6)$$

and

$$A_2 = \frac{1}{i\omega\rho_m} \frac{dP_1}{dx} \frac{(1 - e^{-2h\sqrt{i\omega\rho_m/\mu}})}{e^{-2h\sqrt{i\omega\rho_m/\mu}}(1 - e^{-4h\sqrt{i\omega\rho_m/\mu}})} \quad (7)$$

After these constants are substituted into eqns. (4) and (5), we have,

$$u_1 = \frac{1}{i\omega\rho_m} \frac{dP_1}{dx} \frac{(1 - e^{-2h\sqrt{i\omega\rho_m/\mu}})}{e^{-2h\sqrt{i\omega\rho_m/\mu}}(1 - e^{-4h\sqrt{i\omega\rho_m/\mu}})} [e^{y\sqrt{i\omega\rho_m/\mu}} + e^{-y\sqrt{i\omega\rho_m/\mu}}] \quad \dots\dots\dots (8)$$

Rearranging the above equation, we get,

$$u_1 = \frac{1}{i\omega\rho_m} \frac{dP_1}{dx} \left[ \frac{2(1 - e^{-2h\sqrt{i\omega\rho_m/\mu}})}{e\sqrt{i\omega\rho_m/\mu}(1 - e^{-4h\sqrt{i\omega\rho_m/\mu}})} \cosh(\sqrt{i\omega\rho_m/\mu} y) - 1 \right] \quad (9)$$

## **APPENDIX C**

### **HELIUM**

In the present experiments and analysis, helium was chosen as a medium inside the thermoacoustic tube since helium gas has a low Prandtl number compared to air. The low Prandtl number means that more heat can be transported between the working fluid and the plates. The choice of medium is not restricted to helium-any other fluid which has a low Prandtl number and thus low viscosity and high thermal expansion coefficient can be chosen like liquid metals (liquid sodium,  $Pr=0.004$ ), superfluids  $He^3$ - $He^4$  mixtures ( $Pr=0.1$ ) and other binary monatomic gas mixtures ( $Pr=0.3$ ). Helium was the choice as it is non-toxic, non-flammable and easy to obtain and work with.

Along with the above properties, several other properties will be discussed for better understanding of the reason for helium being selected in the thermoacoustic experiments and analysis. Helium has the lowest melting point of any element and therefore has found wide usage in cryogenic research as its boiling point is close to absolute zero. The conductivity of heat is enormous and increases with temperature and therefore used in the study of superconductivity. Liquid  $He^4$  expands above 2.174 K on cooling. Due to its high conductivity it is used as a cooling medium in nuclear reactors.

The specific heat of helium gas is relatively very high. Since it is monatomic, the gas heat capacities at a given pressure are constant with temperature.

The density of He vapor at the normal boiling point is also very high, with the vapor expanding greatly when heated at room temperature. Also the density of helium is almost twice that of hydrogen. The usefulness of helium depends largely on its extreme properties, for example, its lightness and non-flammability. Above all the Prandtl number of helium is lower than other rare gases.

One of the problems that can be encountered using of helium is its diffusion through most metal and plastic containers under high pressures. Any plastic pressure vessel is more permeable to helium than air at room temperature. The permeability coefficient of helium through the plastic material (Poly-ethyl methacrylate) is  $5.18 \times 10^{-13}$   $\text{cm}^2/(\text{sec} \times \text{Pa})$  at STP. For comparison, the permeability coefficient of neon (Ne) is  $2.28 \times 10^{-13}$  and of oxygen ( $\text{O}_2$ ) is  $0.889 \times 10^{-13}$  (Pauly, 1989). The total permeability of helium through the experimental apparatus is about  $0.3492 \text{ cm}^3/\text{hour}$  and  $0.059 \text{ cm}^3/\text{hour}$  for oxygen. The molecular size of helium is  $0.26 \text{ nm}$ , whereas the oxygen size is  $0.346 \text{ nm}$ .

## **APPENDIX D**

### **THEORY OF ACOUSTICS**

In this section, the basic terms applied either directly or indirectly to thermoacoustics will be described, as a review of acoustics.

Acoustics may be defined as the generation, transmission and reception of energy in the form of vibrational waves in matter. These vibrations are displacements of atoms or molecules of a fluid or solid from their normal configuration. Due to these displacements an internal elastic restoring force arises. The elastic restoring force, coupled with the inertia of the system, enables matter to participate in oscillatory vibrations and thereby generate and transmit acoustic waves. The sound power generally depends upon the environment surrounding the source of sound. This means that sound can be described as a disturbance that propagates through an elastic material at a speed characteristic of that medium.

The thermal effects of acoustic waves have been known for a long time. It is well known that due to the compressions and expansions associated with sound waves, temperature gradients are produced. But these gradients in normal acoustic situations are so small that the thermoacoustic effects are not noticed in everyday life.

Under certain controlled conditions these effects can be enhanced, so that they can be used to refrigerate or produce sound waves in a volume.

There are several papers published to prove the above effects over a period of time. Most of these studies have been from the physics point of view, and lack engineering applications to heat transfer.

Some of the basic terms and equations often used in such studies will be given here.

### **Frequency**

Frequency ( $f$ ) is defined as the number of times per second at which the sound pressure disturbance oscillates between positive and negative values. Frequency above 20000 Hz is termed as ultrasonics and below 20 Hz is infrasonics. It is in this range of 20-20000 Hz which is audible and is normally used in thermoacoustics.

The angular frequency is given by,

$$\omega = 2 \pi f$$

Similarly Period is defined as time required for one complete cycle,

$$\tau = \frac{1}{f}$$

## Wavelength

The wavelength of sound is the distance between analogous points on two successive waves. It is given by,

$$\lambda = \frac{a}{f} = a \tau$$

where  $a$  is speed of sound which depends upon the medium and it is given by,

$$a = \sqrt{\frac{\gamma P_s}{\rho}}$$

where  $P_s$  is the equilibrium gas pressure. In terms of temperature,

$$a = \sqrt{\gamma R T}$$

where  $R$  is the gas constant.

The wave number is defined from the relation,

$$K = \frac{2\pi}{\lambda}$$

## Sound Pressure and Particle Velocity

Most common sounds consist of a rapid, irregular series of positive pressure disturbances (compressions) and negative pressure disturbances (rarefactions) measured from the equilibrium pressure value. The relation of sound pressure is (Kinsler, 1982),

$$P(x, t) = P_L \cos (K(x + ct))$$

where  $t$  is the time,  $P_L$  is the pressure amplitude and  $x$  varies in axial direction.

Every particle has velocity associated with the sound wave in a tube. The relation for the particle velocity and pressure is,

$$u = \frac{P}{\rho a}$$

### **Traveling and Standing Waves**

A wave which is progressive and in which the properties of a particle moving at a velocity change with both time and position is called a travelling wave.

The interference of two waves is called "superposition" and creates a standing wave.

### **Resonance**

Each normal mode of vibration has its own normal frequency (natural frequency). If the source is driven by a steady state generator at specific frequency and if that frequency equals the normal or natural frequency of the enclosure, the sound wave is said to be resonating.